geosciences

Article

Structural Control at Monte Somma and Vesuvio during the Last 5600 Years through Time and Space Distribution of Volcanic Vents

Claudia Principe [1,2,*], Daniele Giordano [1,3], Annarita Paolillo [4], Simone Arrighi [5], Debora Brocchini [6] and Sonia La Felice [1]

[1] Institute of Geosciences and Earth Resources (IGG), National Research Council of Italy (CNR), 56124 Pisa, Italy; daniele.giordano@unito.it (D.G.); sonia.lafelice@igg.cnr.it (S.L.F.)
[2] Vesuvian Observatory, National Institute of Geophysics and Volcanology (INGV), 80124 Naples, Italy
[3] Department of Earth Science, University of Torino, 10125 Torino, Italy
[4] The Italian Institute for Environmental Protection and Research (ISPRA), 00155 Rome, Italy
[5] Department of Earth Science, University of Pisa, 56100 Pisa, Italy; simone.arrighi@unipi.it
[6] Parchi della Val di Cornia S.p.A., 57025 Piombino, Italy; debora.brocchini@parchivaldicornia.it
* Correspondence: c.principe@igg.cnr.it

Abstract: Vesuvio is likely the most if not one of the most dangerous volcanoes in the world. It is an active volcano, quiescent since 1944. The activity of the Monte Somma and Vesuvio volcanic complex is commonly referred to as two central volcanic edifices, namely Monte Somma and Vesuvio. Nevertheless, the opening of numerous eruptive fissures and related vents have characterized Monte Somma and Vesuvio throughout their lives. Spatter cones, spatter ramparts, and related eruptive fissures are disseminated downslope of Vesuvio's main cone and on the southern slopes of the volcano. Similarly, cinder cones, spatter cones, and welded spatters are distributed in the sequence cropping out on the Monte Somma cliff and on the northern slopes of Monte Somma. In this work, a total of 168 eruptive vents have been identified and characterized in a GIS environment in which field data have been merged with relevant information from historical maps and documents. These vents have been arranged into units bounded by unconformities (Unconformity Bounded Stratigraphic Units) defining the eruptive history of the volcano. Alignments of vents and eruptive fissures within each unit have been compared with regional tectonic elements and the volcano-tectonic features affecting Monte Somma and Vesuvio during the last 5600 years, thus inferring that different structural trends were active in the different stratigraphic units. In particular, we show that the N300°–320° regional, Apennine, left-lateral, strike-slip fault system, the N040°–055° Torre del Greco direct fault system, the N70° and the EW fault system, and the generally NS oriented group of local brittle elements, all analyzed here, were differently active during the investigated time span. These tectonic trends might control the position of the eruptive fissures and vents in case of future unrest of the volcano.

Keywords: Monte Somma; Vesuvio; monogenetic vents; fissure eruptions; tectonic trends

Citation: Principe, C.; Giordano, D.; Paolillo, A.; Arrighi, S.; Brocchini, D.; La Felice, S. Structural Control at Monte Somma and Vesuvio during the Last 5600 Years through Time and Space Distribution of Volcanic Vents. *Geosciences* **2024**, *14*, 91. https://doi.org/10.3390/geosciences14040091

Academic Editors: Jesus Martinez-Frias and Karoly Nemeth

Received: 15 January 2024
Revised: 10 March 2024
Accepted: 11 March 2024
Published: 22 March 2024

1. Introduction

More than 800,000 people live in the area surrounding Vesuvio, which has been deeply impacted by large effusive and explosive eruptions. The occurrence of flank eruptions during Vesuvio's volcanic history has been largely underestimated in the previous literature e.g., [1]. Previous studies and maps—including two large-scale geological maps [2,3]; the geological and volcano-tectonic map creates by [4]; and the lineaments' sketch maps drafted by [5,6]—all limit monogenetic vents and eruptive fissures to a restricted set. This set is commonly identified by (i) a few volcanic centers preceding the AD 79 eruption (e.g., at Camaldoli della Torre, Strocchioni, Pollena, and San Severino); (ii) the lava domes and vents produced during the post-1631 mixed activity (i.e., partly explosive and partly effusive also during the same event) and mainly located within the summit caldera area (e.g., Colle Umberto, Colle Margherita, 1906); (iii) the eruptive fractures which opened during the Vesuvio historical activity within the main cone (Gran Cono Vesuviano); (iv) the Viulo and the Fossa Monaca Middle Age lava flows as well as the 1760, 1794, and 1861 monogenetic vents.

Furthermore, the Vesuvio volcano has been so far affected by a substantial lack of attention toward the description of brittle structural elements, i.e., faults and fractures, even within geological maps, such as those of [2,3,7]. In recent times, predictive studies and models of Monte Somma and Vesuvio were produced, considering either a few tectonic features only [8–11] or volcano-tectonic characteristics only, such as caldera and flank collapses e.g., [12]. Finally, only the few monogenetic vents and eruptive fissures recognized by previous works were considered in the studies of [13,14].

Up to now, only the investigations of [15,16], first, and the work of [17] for the south-western sector of the volcano, second, showed that fast-moving lava flows were erupted in historical times from previously unnoticed monogenetic vents and fissures, which follow tectonic trends of regional and/or local importance. As a natural continuation of these studies, in the present contribution, we show how the clustering, in time and space, of flank eruptions (much more than those recognized in the previous literature) has been controlled by structural and volcano-tectonic trends and has affected the activity of the Monte Somma and Vesuvio volcanic complex during the last 5600 years. Older Monte Somma monogenetic eruptive centers have been also considered here in order to provide a more complete and detailed analysis of the structural pattern of the whole volcanic area. Our work is based on a detailed and new fieldwork focused on defining the cartography of volcanic deposits and tectonic and volcano-tectonic elements at the scale 1:5000. Our work is also supported by the census and critical analysis of historical sources. In fact, the writings and maps produced simultaneously or shortly after the eruptions contain descriptions and representations of the places in which eruptive fissures opened and/or vents were formed, which greatly helped in the accurate positioning and age attribution of a substantially larger number of eruptive vents than in the previous literature (Appendix A). Finally, our assessment of the locations of historical eruptive features at Vesuvio and the correlation of vent locations with regional structures expounds the likely style of future eruptive activity and hypothesizes its most likely location.

2. Stratigraphical Outline

The Monte Somma and Vesuvio volcanic complex is a moderate-sized stratovolcano with an altitude of 1281 m above sea level, located along the Gulf of Naples coastline, in the southernmost portion of the Campanian Plain (Figure 1). It consists of the remnants of the Monte Somma poly-phased caldera [12] surrounding the Vesuvio cone (Gran Cono Vesuviano), whose summit crater is about 500 m in diameter [18].

Recently, [17] mapped the south-western sector of the volcano and subdivided the whole Monte Somma and Vesuvio stratigraphy into Unconformity Bounded Stratigraphic Units (UBSU; Table 1), according to the groundbreaking criteria established by [19]. These units are identified and separated by different types of unconformities such as angular unconformities, erosional surfaces, disconformities (i.e., irregular or uneven erosion surfaces or indications of weathering in essentially parallel bedding), and soils when corresponding to a significant depositional *hiatus* in the stratigraphic succession. This approach differs from the previously used methods which divided the Monte Somma and Vesuvio activity into cycles of activity, eruptive units, or time periods between Plinian eruptions, and is nowadays recognized as an objective manner to distinguish volcanic phases on the basis of reproducible field characteristics, while also considering the geological (in the sense of non-volcanological) events that occurred inside and/or at the limit of a given volcanic area.

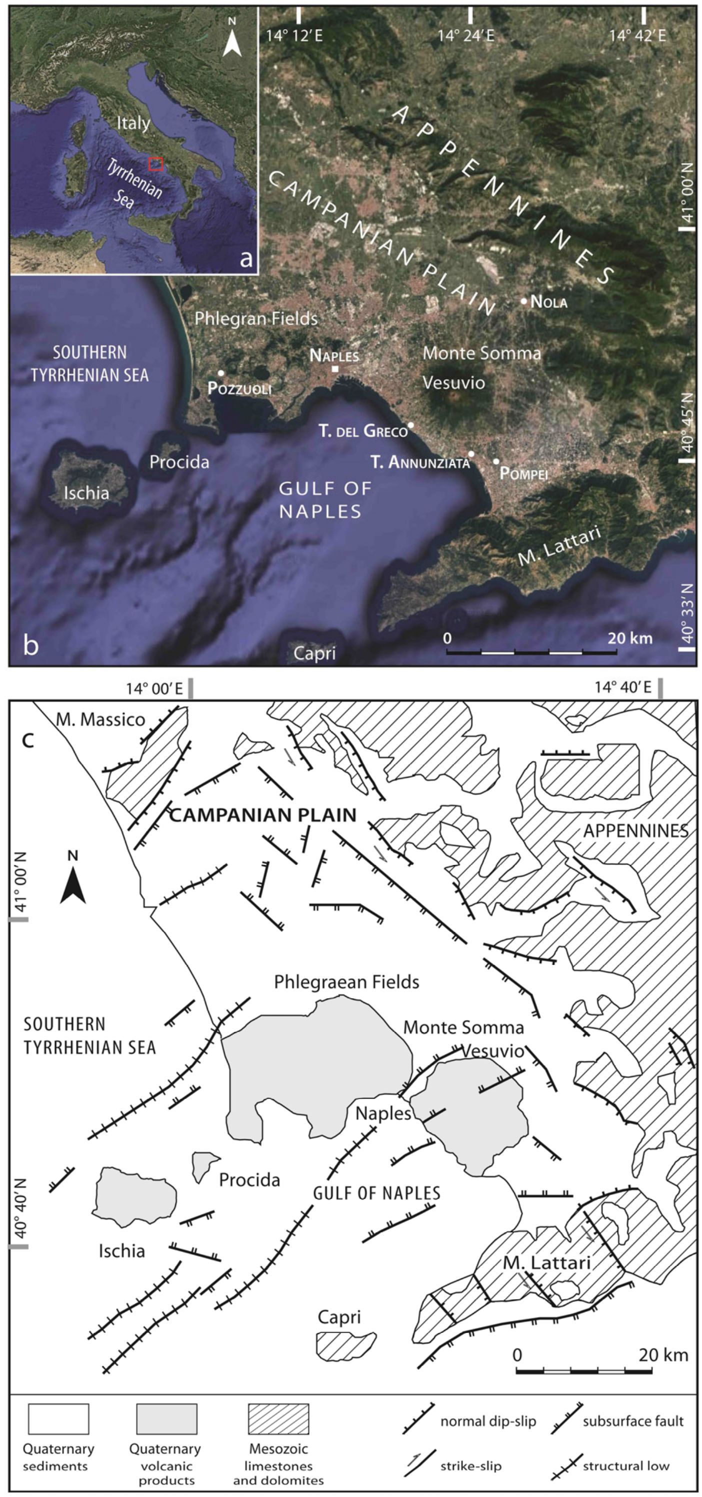

Figure 1. (**a**,**b**) Location of the study area and (**c**) geotectonic sketch map (modified from [17]).

Accordingly, the Vesuvio activity in the last 5600 years falls within the Vesuvio Super-Synthem (Figure 2), whose base is represented by the discontinuity surface originating after the Versilian Transgression, dated at about 5600 years BP. Minor discontinuities separate the other six synthems (Table 1) grouped in the Vesuvio Super-Synthem.

Table 1. Monte Somma and Vesuvio synthematic stratigraphy, modified from [17]. PF: eruption from Phlegraean Field.

Top discontinuity: in development from the last eruption in 1944

Vesuvio Super-Synthem (Present – 5600 a BP)

Present Vesuvius Synthem (1944 - 1631)
- Piano delle Ginestre Sub-Synthem (effusive and mixed eruptions mild eruptions)
- 1631 eruption Sub-Synthem (Plinian eruption/summit collapse)

(m) Second order discontinuity: eruptive stasis

Medieval Vesuvius Synthem (1139-AD 472)
- Miglio d'Oro Sub-Synthem (tectonic phase/paleosol)

(l) Second order discontinuity: erosive surface/new hydrography

Ancient Vesuvius Synthem (AD 472-AD 79)
- AD 472 eruption Sub-Synthem (summit collapse)
- Late Antique period (AD 203 eruption, etc. . .)

(i) Second order discontinuity: erosive surface/new hydrography

Proto Vesuvius Synthem (AD 79 – 4000 a BP)
- AD 79 eruption Sub-Synthem (Plinian eruption/caldera)
- Pre-Roman Sub-Synthem (AP explosive eruptions, Civita di Pompei, Camaldoli, T. Bassano lateral vents)

(h) Second order discontinuity: eruptive stasis

Prehistoric Vesuvius Synthem (4000 a BP – 5600 a BP)
- Avellino eruption Sub-Synthem (4000 a BP) (sector collapse/tuff-cone edifice)
- PF → "Agnano Monte Spina" eruption

(G) First order discontinuity: Versilian marine transgression at about 5600 years BP

Somma Super-Synthem (5600 – 25,000 a BP)

- «Mercato» eruption Sub-Synthem (8900 a BP) (caldera/paleosol)
- PF → "Lagno Amendolare" eruption

(f) Second order discontinuity: glacial fluctuation phase (12,000 a BP)

Cognoli di Levante Synthem (lava edifice)

(e) Second order discontinuity: glacial fluctuation phase (18-19,000 a BP)

Cognoli di Ottaviano Synthem
- "Greenish pumice" eruption Sub-Synthem (19,200 a BP)(Plinian eruption/caldera)
- Punta del Nasone Sub-Synthem (welded spatter/tectonic phase)
- Canale dell'Arena Sub-Synthem (cinder cone edifice)
- Cognoli di Sant'Anastasia Sub-Synthem (glacial till)

(d) Second order discontinuity: second deglaciation phase (21-22,000 a BP)

Pomici di Base Synthem
- Brown Chocolate Sub-Synthem (tuff-cone edifice)
- PdB eruption Sub-Synthem (22,000 a BP) (sector collapse)

(C) First order discontinuity: Regional erosive surface under "Pomici di Base" eruption deposits, first and major deglaciation phase post-LGM, at 25-26,000 a BP

Proto Somma Super-synthem (25,000 – 39,000 BP)

Cognoli di Trocchia Synthem (lava edifice)
- PF → "Codola" pumice eruption

(b) Second order discontinuity: erosive surface

Trapolino Synthem (welded spatters/lateral vents)

(A) First order discontinuity: erosive surface on top of the Campanian Ignimbrite

PF → "Campanian Ignimbrite" eruption

The other two super-synthems that constitute the stratigraphy of this volcanic area are the Somma Super-Synthem (between 5600 years BP and 25,000 years BP) and the Proto Somma Super-Synthem (between 25,000 years BP and 39,000 years BP), which are defined by the regional erosive surfaces at the top of the *Pomici di Base* Plinian eruption deposits and at the top of the Campanian Ignimbrite deposits, respectively (Table 1).

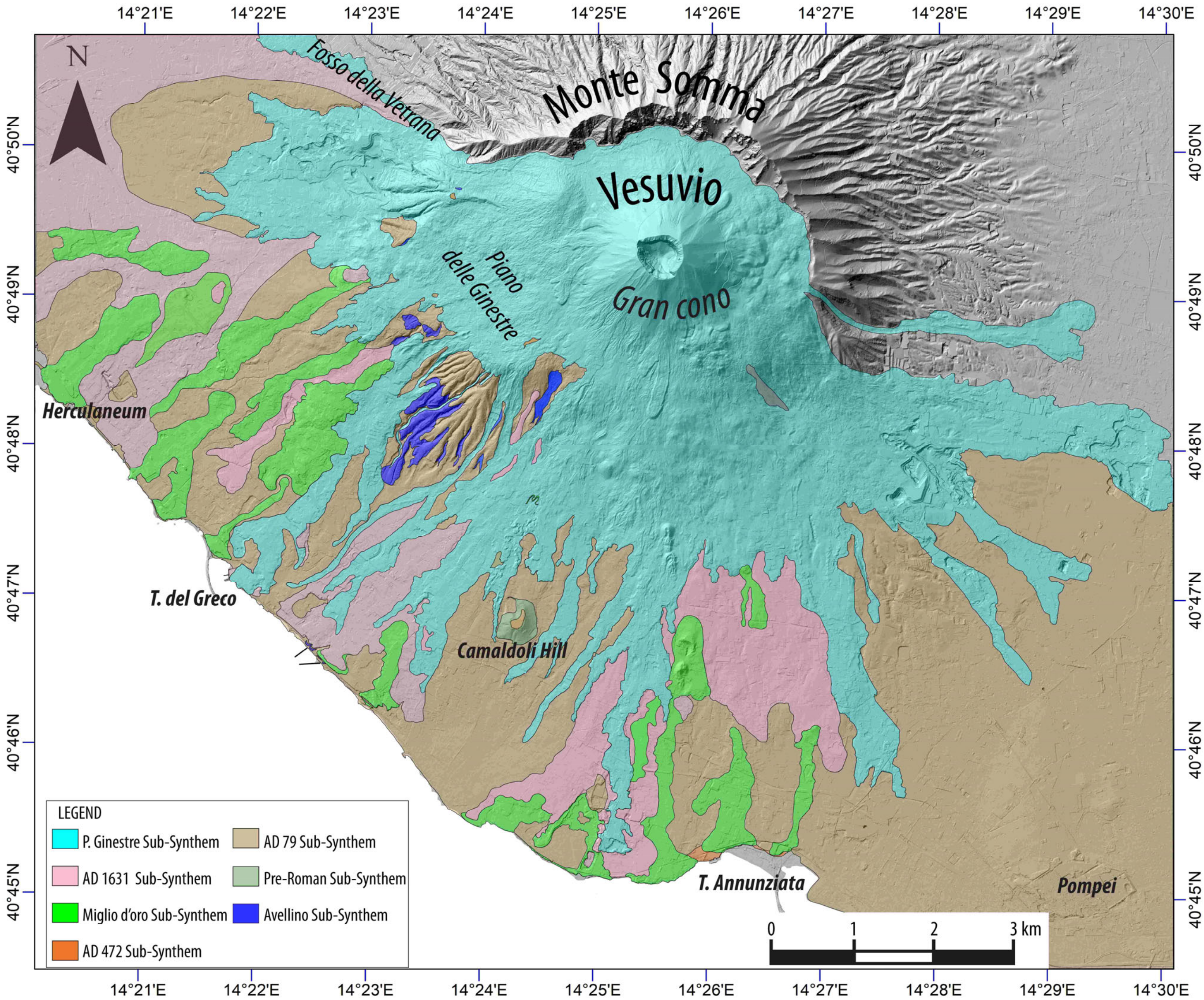

Figure 2. Synthematic geological map of Vesuvio from [17] and the new survey of volcanic deposits performed in this work at the scale 1:5000. Digital Elevation Model (DEM) from the *Regione Campania* database.

3. Regional Tectonic Framework and Previous Structural and Morpho-Structural Studies

The occurrence of Campanian volcanoes is limited to the north and to the south by the regional structural trends of the 41st and 40th parallels (Figure 1). Within this area, the Monte Somma and Vesuvio volcanic complex is positioned at the intersection of two regional fault systems striking NW-SE and NE-SW e.g., [20–27]. Based on seismological data, Finetti and Morelli [20] suggested, for the first time, that the presence of the NE-SW direct, regional fault affects the Mesozoic carbonate basement of the volcano and continues in the Apennine chain (Figure 1). According to these authors, this low-angle active fault system cut the volcanic edifice in correspondence of the Torre del Greco and Torre Annunziata towns.

Other studies based on the analysis of seismic focal mechanisms, shear wave splitting, and meso-structural data indicate the occurrence of a generically indicated NW-SE trending oblique-slip fault system which intersected the Gran Cono Vesuviano and the Plio–Quaternary sediments of the Campanian Plain [5,24,28].

On the other hand, [29] showed that an additional NE trending normal fault system and a WNW-ESE directed fold system were active in the Late Qua ternary.

Focusing on the volcano, [2], in their map at the scale 1:25,000, reported the feeding fractures of Viulo-Fossa Monaca medieval lava flows (N345°), the 1760 lava flows (both N15° trending), and the ones feeding the 1794 lavas (N82° trending) and the 1861 lavas (N66° trending) only, without providing for them any specific kinematic context. The same authors, and later Sbrana et al. (2020), identified for Monte Somma the three linear elements of Lagno di Pollena, Cupa dell'Olivella (both N300° trending), and Vallone San Severino (N55° trending) only as simple fractures, with no particular association to any local or regional-scale fault system.

More recently, [9] modeled the directions of a few apical fractures cutting the main cone and feeding Vesuvio's effusive activity, while [10,11,30] studied the geometric and kinematic features of Monte Somma dikes [13,14] reviewed the position of the onland vents recognized in the previous literature. Based on geophysical studies, [31–33] identified the position of offshore vents. Finally, structural elements such as faults, fractures, and geomorphological features were measured by [11]. According to these authors, the Apennine (NW-SE) and anti-Apennine (NE-SW) trends prevail in rocks older than the AD 79 eruption and at distance > 2 km from the Gran Cono Vesuviano, while NS and EW local-scale fragile elements affect the younger volcanic units.

To sum up, various approaches focusing on the description of different morphological, structural, and phenomenological aspects, mostly at the local scale, were adopted in previous works, but none of them have yet provided a complete cartographic tool synthesizing the relationships amongst vent distribution, regional tectonic trends, and regional and local-scale volcano-tectonic features.

Based on our studies [15–17], in the Monte Somma and Vesuvio area, five main fault systems, identified on the basis of morpho-structural and stratigraphic evidence, were active in the last 5600 years: (i) the N300°–320° regional, Apennine, left-lateral, strike-slip fault system, (ii) the N40°–55° Torre del Greco direct fault system, (iii) the N70° fault system, (iv) the EW fault system, and (v) the generally NS oriented group of local brittle elements. For instance, the combined action of both the N300°–320° and the N40°–55° fault systems were responsible for the two sector collapses related to the Plinian eruptions of the *Pomici di Base* and *Pomici di Avellino* and are deeply involved in the formation of the Monte Somma cliff [34].

Finally, our geomorphological, chrono-stratigraphic, and cartographic studies highlight the presence of several, previously unknown, Middle Age eruptive fissures and linear volcano-tectonic features with displacements of tens to hundreds of meters both on Monte Somma and Vesuvio edifices [15–17]. These lineaments are related both to the N300°–320° regional Apennine fault system and the N040°-055° fault system—corresponding to the "Torre del Greco fault" of [20]—and the N70° fault system [17].

4. Methods and Results

The Shaded Relief Map derived from the Digital Elevation Model (DEM), with a spatial resolution of 1 m, obtained from LiDAR data by the *Regione Campania* and made available by the *Ministero dell'Ambiente e della Tutela del Territorio e del Mare*, has been adopted here. The position and direction of the structural and volcanological elements analyzed in this work, both newly identified and reported in previous studies, have been reported on this Shaded Relief Map.

Toponyms and other features (such as roads, palaces, churches, and archaeological sites), useful for ascertaining the age of volcanic activity, have been retrieved from the analysis of the 1:5000 scale topographic maps produced by *Cassa del Mezzogiorno* (southern Italy development agency, 1978). Toponymy is important everywhere because the place names are generally assigned on the basis of specific morphological features or for historical reasons. Toponymy is especially important in areas affected by intense volcanism, such as Monte Somma and Vesuvio, where the succession of eruptive events causes continuous changes in morphology and consequent changes in the names of geographic features. For example, the present location of the Railway Museum of *Pietrarsa* (which is Italian for "burned stone"), near Portici, takes its name from the effects of the 1631 eruption, whose pyroclastic flow deposits covered this promontory (Figure 2). Prior to this eruption, this locality was known by the name of *Pietrabianca* (which is Italian for "white stone"), due to the whitish color of the pyroclastic flow deposits of the *Pompei* eruption which formed this promontory in AD 79 [35,36]. As another example, some places on the Vesuvio slopes are called "Tironi" or "Monteroni". The term "Tironi" is the late-Latin language deformation of the geometrical term "torus", a sort of donut-shaped surface. Similarly, the term "Monteroni" is a tautology composed of the Italian term "monte" (which is mons in Latin and hill in English) and "Tironi". Both "Tironi"and "Monteroni" have the meaning of a hill with toroidal shape [37]. Interestingly, we discovered that the hills with these names were scoria cones from which lava flows originated, as already observed by some ancient authors in some cases e.g., [38].

Many of the vents produced during historical eruptions are today buried under the most recent lava flows and pyroclastic covers. Some of these vents are described in the numerous historical accounts of the events which occurred after the 1631 eruption [39] (https://geca-cnr.ge.imati.cnr.it/pisa/vulcani/make_home_page.php?status=startdv accessed on 14 January 2024) and, in the luckiest cases, reported in ancient topographical maps. A number of these topographies are still preserved in the historic libraries of the Vesuvian Observatory, the Storia Patria Society, and the National Library in Naples, as well as in some other Italian and foreign libraries such as those of the *Istituto Geografico Militare* (IGM) in Florence, the *Istituto Superiore per la Protezione e la Ricerca Ambientale* (ISPRA) in Rome, and the University College London. Old maps were scanned at high resolution, georeferenced with the Ground Control Points' method, compared with each other, and then overlaid onto the adopted Shaded Relief Map, using the WGS84 UTM 33N, by means of GIS standard tools. Of particular relevance are the topographic map of [40], the geological map of [41], and the topographic surveys of the intra-caldera area performed before and after the 1906 eruption by [42,43]. The numerous vents reported in these ancient maps were field checked in this work. We anticipated that the ages attributed by the ancient authors resulted in fitting with our stratigraphic reconstruction (Figure 3). The newly discovered vents were geographically located in the field using a GPS Garmin GPSMAP64s instrument and stratigraphically positioned.

Maps of hydrographic catchments and topographic slopes have been produced by use of the GIS instrument Esri Arc-GIS^{TM}. These maps highlighting morphological patterns and anomalies—such as alignments of eruptive vents, drainage irregularities, fault lines, and coastline morphology—have been field checked and used to define kinematic indicators of structural patterns. Geometric and stratigraphic relationships between volcanic deposits of different facies and defined structural elements have been used to stratigraphically constrain the activity of structural trends.

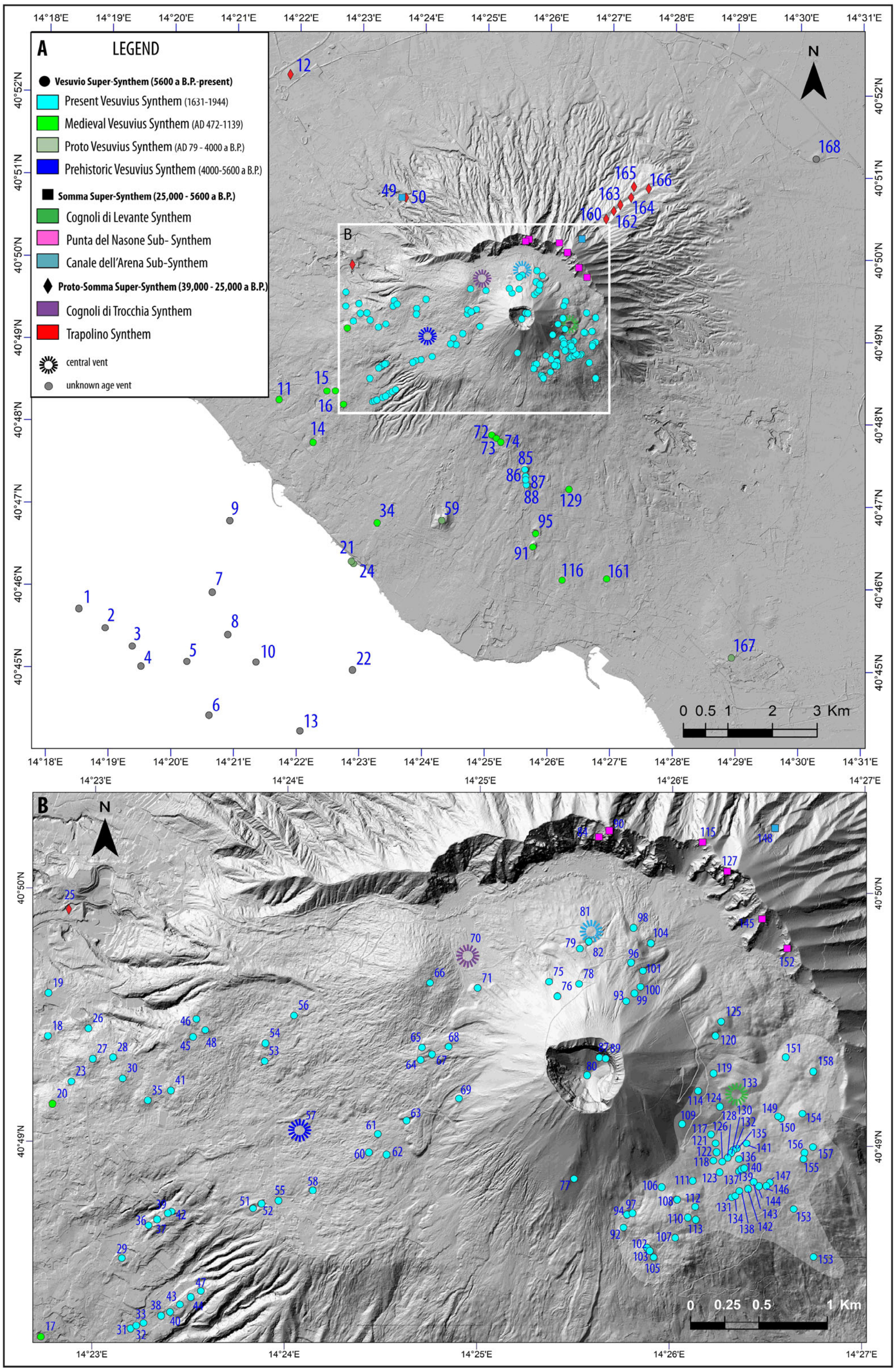

Figure 3. Distribution of Monte Somma and Vesuvio vents. (**A**) Eruptive vents identified on the volcanic edifice and offshore. (**B**) Eruptive vents identified in the central portion of the volcanic edifice. Vents are numbered from left to right. Numbers refer to the description of vents given in Appendix A and colors refer to the synthematic stratigraphy in Table 1. DEM from the *Regione Campania* database.

5. Distribution of Vents in Time and Space and Relationship with Structural Trends

The distribution of Monte Somma and Vesuvio monogenetic vents is reported in Figure 3, while their main features are shown in Appendix A (In Appendix A, all names of the cited locations refer to a number in Figure 3 and coordinates are given.). In the south-western and southern sectors of Vesuvio, vent structures and fragile elements are easily recognizable because the outcropping deposits are mainly the lava flows stratigraphically overlying the tephra of the *Pomici di Avellino* and Pompei AD 79 explosive eruptions (Figure 2 and Table 1). In the easternmost sector of Vesuvio, faults, eruptive fractures, and vents were detected under a few-meters-thick lapilli cover produced by the Present Vesuvius Synthem explosive activity with NE and SE dispersion axes [44].

All of the 168 vents considered in this work (Appendix A), including those already known and the new ones, have been stratigraphically positioned and related to the brittle elements defined here, integrating historical data and fieldwork analysis. As expected, the greatest concentration of vents is found in the intra-caldera area, even if they are spread over the entire Monte Somma and Vesuvio volcanic complex (Figure 3). Of course, the total number of eruptive centers are underestimated in that an undefined number of vents were destroyed or buried by the subsequent volcanic activity.

For the central part of the volcano, brittle elements—defined on the basis of morphological and stratigraphical evidence—have been reported together with eruptive fissures (Figure 4) to distinguish purely structural (non-eruptive) elements from volcano-tectonic (eruptive) features. The oldest vents are positioned on the Monte Somma slopes (Case Sorrentino-N. 25, Trapolino quarry-N. 165, Pollena quarry-N. 49 and N. 50, and Vallone San Severino-N. 148, 160, and 162–166) and were active during the Proto Somma and Somma Super-Synthems (Table 1). In the case of Vallone San Severino, vents are clearly aligned along the N040°–055° direction (Figure 3).

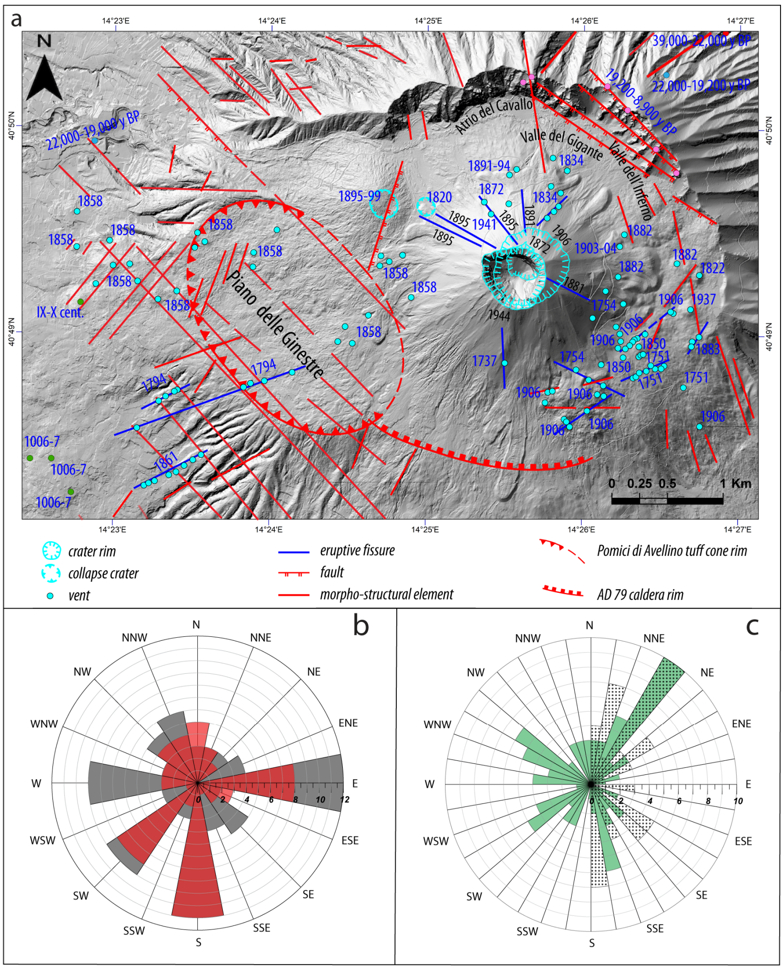

Figure 4. (**a**) Shaded Relief Model of the central portion of the volcano showing vents (symbols and colors as in Figure 3) with age attribution, eruptive fissures (in blue), and fragile elements (in red). DEM

from *Regione Campania* database. (**b**) Rose diagram of the eruptive fissures on the *Gran Cono Vesuviano* based on the 85 data points from [45] (dark grey) and the 61 data points from [46] (red), which are in good agreement with each other. (**c**) Rose diagram of the Monte Somma cliff dykes comprising 98 elements from [30] (green color) and 68 elements from [4] (polka dots). The prevailing trends in both rose diagrams are N300°–320°, N040°–055°, ca. NS, and ca. EW.

5.1. Vents Formed during the Pre-Historic Vesuvius Synthem (4000 a BP–5600 a BP)

The Pre-Historic Vesuvius Synthem includes the Avellino eruption Sub-Synthem made of the *Pomici di Avellino* deposits (1995 ± 10 calBC, [47]). A tuff cone was built in the last phases of the *Pomici di Avellino* eruption [17]. The tuff cone is still morphologically evident and has been labeled as a central vent with the N. 57 in Figure 3. The tuff cone crater is clearly modeled by tectonic elements of the N300°–320° regional fault system (Figure 4).

5.2. Vents Formed during the Proto Vesuvius Synthem (AD 79—4000 a BP)

The Proto Vesuvius Synthem includes two sub-synthems. The Pre-Roman Sub-Synthem includes the eruptive deposits between AD 79 and the *Pomici di Avellino* eruptions, while the AD 79 eruption Sub-Synthem is made up of the Pompei eruption deposits (Table 1). Also belonging to the Pre-Roman Sub-Synthem, there are the Camaldoli della Torre cinder cone and the Civita di Pompei lava vent (respectively, N. 59 and N. 167 in Figure 3), both positioned in the SE sector of Vesuvio. The Camaldoli della Torre cinder cone (Figure 5b) is made up of a succession of lavas and coarse scoria beds; these deposits lay under the Pompei deposits and are underlain by the *Pomici di Avellino* [48]. The modest relief of the Civita di Pompei hill (54 m a.s.l.), on which the Roman city of Pompei destroyed by the AD 79 eruption was built, is a volcanic center made up of welded spatters and short lava flows [49], positioned at the SE outskirts of the Gran Cono Vesuviano (N. 167 in Figure 3). Due to the lack of the *Pomici di Avellino* deposits [50] in the stratigraphic sequence between the Pompei pyroclastics and the lavas of the Civita di Pompei center e.g., [51,52], this eruptive center is placed within the Proto Vesuvius Synthem (Table 1).

At the sea cliff between the Torre Bassano and the semi-submerged archaeological site of Villa Sora-Ponte di Rivieccio, there are two vents (N. 21 and N. 24 in Figure 3a) aligned AT N300°–320° and already recognized in the previous literature [41,53]. Today, these vents are practically no longer visible due to marine erosion and the construction of numerous human settlements. These deposits were photographed and described by [54] as sub-aerial aphanitic lavas and welded scoriae from a local lenticular-shaped vent, approximately 100 m long and with a maximum exposed thickness of about 4–5 m, cropping out along the sea cliff. They are covered by diluted pyroclastic density current deposits (i.e., surges) of the Pompei AD 79 eruption [54], but at places (e.g., Ponte di Rivieccio), they are described to overlay "paleosols and rests of pumice deposits", possibly referable to the AP eruptions. The AP1 to AP6 events are small to medium-sized explosive eruptions which occurred between the *Pomici di Avellino* and the *Pompei* (AD 79) Plinian eruptions and were described for the first time by [55]. Therefore, these vents have also been attributed to the Proto Vesuvius Synthem.

A Pompei fresco reveals the presence of two vents within the depression of the Piano delle Ginestre, which represents what remains of the crater left by the last phases of the *Pomici di Avellino* eruption [56]. These two vents, with a generic NW-SE alignment, have been attributed to the cited AP explosive eruptions, but they are not reported in Figures 3 and 4 and in Appendix A due to the uncertain location.

The main eruptive episode in this period is represented by the Pompei AD 79 eruption, whose deposits shaped volcano morphology (Figure 4). The eruption was generated from the central edifice of Cognoli di Levante (Somma Super-Synthem, Cognoli di Levante Synthem in Table 1), which was partially destroyed by the AD 79 caldera collapse [56]. The hypothetical position of the central vent of the Cognoli di Levante edifice is reported in Figure 3 (vent N. 133).

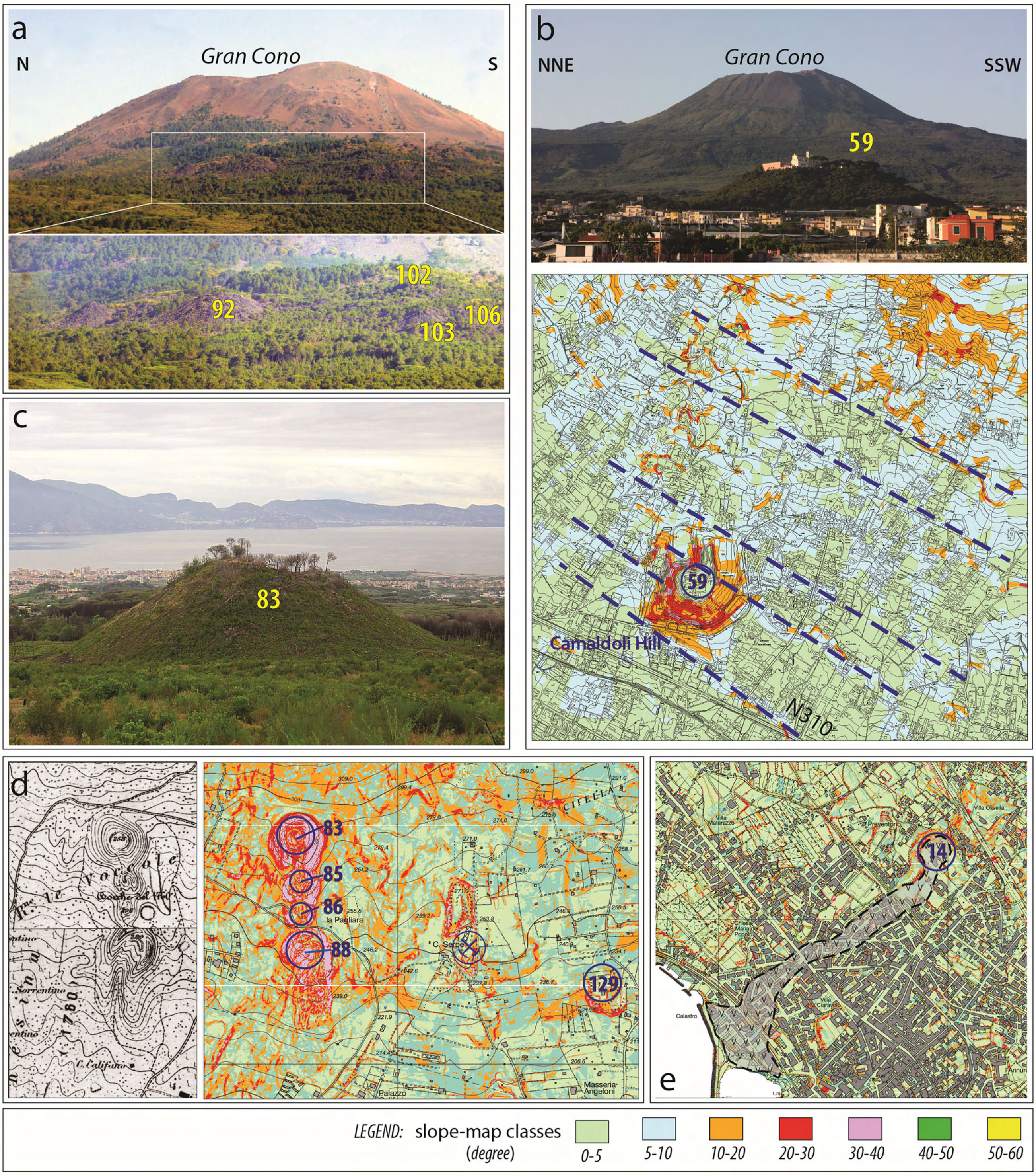

Figure 5. Images of the monogenetic vents punctuating Vesuvius slopes. Vent numbers are those reported in Appendix A and Figure 3. (**a**) The vents of the 1906 eruption at the foot of the Gran Cono Vesuviano. (**b**) The Camaldoli hill cinder cone in a photograph from the south and in the slope-map generated from the *Regione Campania* database. The slope map highlights a number of morphological N300°–320°-trending elements in the Camaldoli area. (**c**) The evident cone morphology of the northernmost 1760 vent as a result of the loss of vegetation due to the fire of the summer 2017 (photo by Gino Scarpato). (**d**) Vents of the 1760 lava flow in (**left**) the [40] topographic map and (**right**) the slope map generated in this work, in both of which the morphology of the main 4 vents is still evident. (**e**) Vent and lava field of the Calastro medieval eruption, both within the present-day Torre del Greco town.

5.3. Vents Formed during the Ancient Vesuvius Synthem (AD 472–AD 79)

In the period between the main explosive eruptions of AD 79 and AD 472, a mild explosive activity took place [15,18,41,57–60]. According to [61], a main Vesuvio central cone was built in the AD 79–AD 472 interval and was beheaded at the end of the AD 472 eruption. However, in this work, it was not possible to recognize the vent of the AD 472 eruption.

5.4. Vents Formed during the Medieval Vesuvius Synthem (1139—AD 472)

During the Middle Age, volcanic activity consisted mainly of lava flows emitted from monogenetic vents and comprised also a black lapilli fallout related to the 1139 eruption [15]. These vents are few-tens-of-meters-high coalescent spatter cones located on the southern slopes of the Gran Cono Vesuviano (Figure 3).

The comparison between recent and ancient photographs and documents has highlighted how some vents of this period were completely buried or removed by recent anthropic action. This is the case of the vents of the Tironi lava field which were mapped by [17] and previously described by ([37], pages 39 and 84). This author showed that these spatter cones were aligned in an approximately NNE direction and coalesced along an eruptive fracture, and reported the occurrence of both "deep cavities" and "gas emissions".

A total of 15 medieval vents have been positioned in this work, as reported in Figure 3. Most medieval vents are controlled by the N300°–320° regional fault system [16].

5.5. Vents Formed during the Present Vesuvius Synthem (1944–1631)

An eruptive stasis ensued after 1139 and ended with a small-scale Plinian eruption in 1631 that destroyed the Gran Cono Vesuviano present at that time. The summit was rebuilt over the following centuries by mild effusive and explosive strombolian activity that ended in 1944 [18,44,62,63]. During the time interval between 1631 and 1944—generally known as the recent period of Vesuvio activity in the literature e.g., [64]—numerous eruptive fissures opened into the Gran Cono Vesuviano. These fissures gave rise to several lava flows spreading on the southern slopes of the volcano (Figure 2). In the past, various authors attempted to position eruptive fissures and vents of this period based on historical documents [8,45,46,62,65], but these exercises were incomplete and, in some cases, misleading, without field-checking. The eruptive fissures still visible on the *Gran Cono Vesuviano* and those marked in the historical maps are reported in Figure 4a, whereas all data from historical chronicles are listed in Table 2 and shown in the rose diagram of Figure 4b. Unfortunately, it was not possible to consider the length of the fissures in Figure 4b, as this parameter is not reported in historical sources. The prevailing trends in this rose diagram are N300°–320°, N040°–055°, ca. NS, and ca. EW. During some eruptions (e.g., in 1737, 1822, and 1906) of this period characterized by open-conduit and semi-persistent activity, the Gran Cono Vesuviano was cut from side to side by eruptive fissures, whose directions have been recorded in ancient studies.

During the Present Vesuvius Synthem, lavas and pyroclastic products of the eruptions of this last period of activity accumulated inside the caldera formed by the Pompei AD 79 eruption and in the Piano delle Ginestre. Reported in Figure 4a is the distribution of 115 vents that were active in this interval of time both downslope of the Gran Cono Vesuviano and inside and outside the Piano delle Ginestre and the AD 79 caldera rim. These vents generally are aligned on different eruptive fissures belonging to the same trend. This is the case of the 1906 eruption [66,67], with 20 vents aligned N040°–055°, and of the 1858 eruption [68], with 24 vents positioned along the same tectonic trend on the eastern slopes of the Avellino tuff cone (Figure 4).

During the three and a half centuries following the 1631 eruption, the Gran Cono Vesuviano experienced periods of building, interrupted by beheading episodes at the end of major eruptions [69]. Of particular importance are the collapses of the upper portion of the main cone which occurred at the end of Sub-Plinian eruptions with phreatomagmatic components [44]. Traces of the last three collapses, dated 1872, 1906, and 1944, are still visible today and have been reported in Figure 4 from the [40,42,43] maps.

Table 2. Directions of eruptive fissures on the Gran Cono Vesuviano during the last period of activity (1631–1944). Data from [45,46], and the present study. Some eruptions show more than one eruptive fissure.

	DIRECTION															
ERUPTION	**N**	**NNE**	**NE**	**ENE**	**E**	**ESE**	**SE**	**SSE**	**S**	**SSW**	**SW**	**WSW**	**W**	**WNW**	**NW**	**NNW**
1698–99											•					
1701						•										
1707											•					
1714									•							
1717											•					
1723													•			
1724–26									•							
1730						•										
1737			•							•						
1751								•								
1754					•											
1760									•							
1767	•								•							
1771	•															
1779		•							•							
1786	•															
1790											•					
1794												•				
1804					•								•			
1805											•					
1806											•					
1813					•											
1817			•													
1820														•		
1821														•		
1822						•										
1833									•							
1834															•	•
1839					•								•			
1847										•						
1850		•			•											
1855	•															
1858	•				•											
1861											•					
1868					•										•	•
1872									•							

Table 2. *Cont.*

		DIRECTION															
		N	**NNE**	**NE**	**ENE**	**E**	**ESE**	**SE**	**SSE**	**S**	**SSW**	**SW**	**WSW**	**W**	**WNW**	**NW**	**NNW**
ERUPTION	**1881**					•											
	1882							•									
	1885									•							
	1891									•						•	•
	1895							•							•		
	1903																
	1905															•	•
	1906		•							•							

Only a few well-known vents have been recognized outside the summit portion of the volcano during the Present Vesuvius period of activity (Figure 3). These vents gave origin to the 1760, 1794, and 1861 lava flows [2,62] which reached the coast and affected the territories and towns of Torre del Greco and Torre Annunziata. In the 1760 eruption, 15 vents opened [70] (Figure 6) at a distance of about 4 km from the central Vesuvio crater and 4 km from the coast. The four most active of these vents [70] are still evident (Figure 5c,d). These vents, aligned on an NNW-oriented eruptive fissure (Figure 5), emitted lava flows that reached the coast [2]. During the 1794 eruption, lava flows were emitted by seven vents aligned on N070°-striking eruptive fractures (Figure 4), located at a distance of about 3 km from the central Vesuvio vent and 4 km from the coast (Figure 3). The lava flows destroyed a great portion of Torre del Greco, currently the third largest town of the Campania region. In the same period, the main crater was also active [44] and the main cone was entirely crosscut by an N70°-trending fault system, while four additional vents on the eastern portion of this fissure produced a second lava flow which ran eastwards [71,72]. During the 1861 eruption, 11 spatter cones opened to the south of the 1794 lower vents (Figure 7). Also, in this case, the vents were all aligned on a well-defined N070° eruptive fissure. During this eruption, a series of earthquakes occurred, accompanied by the opening—from the end of the eruptive fissure into the sea—of a curtain of fractures aligned N040°–055° and characterized by strong fluid emission [17,73]. Not as well-known as the previous cases is the eruptive fissure that opened during the 1872 eruption [74]. The eruptive fissure, oriented N070°, cut the *Gran Cono* of Vesuvio from top to bottom, starting from a pre-existing parasitic vent on the summit crater rim (Figure 8).

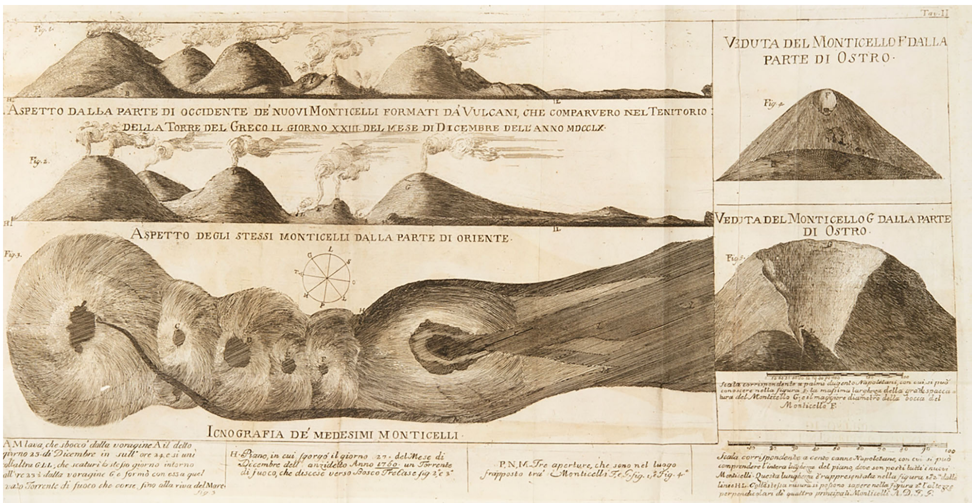

Figure 6. Representation of the vents of the 1760 Vesuvius eruption as given by [70].

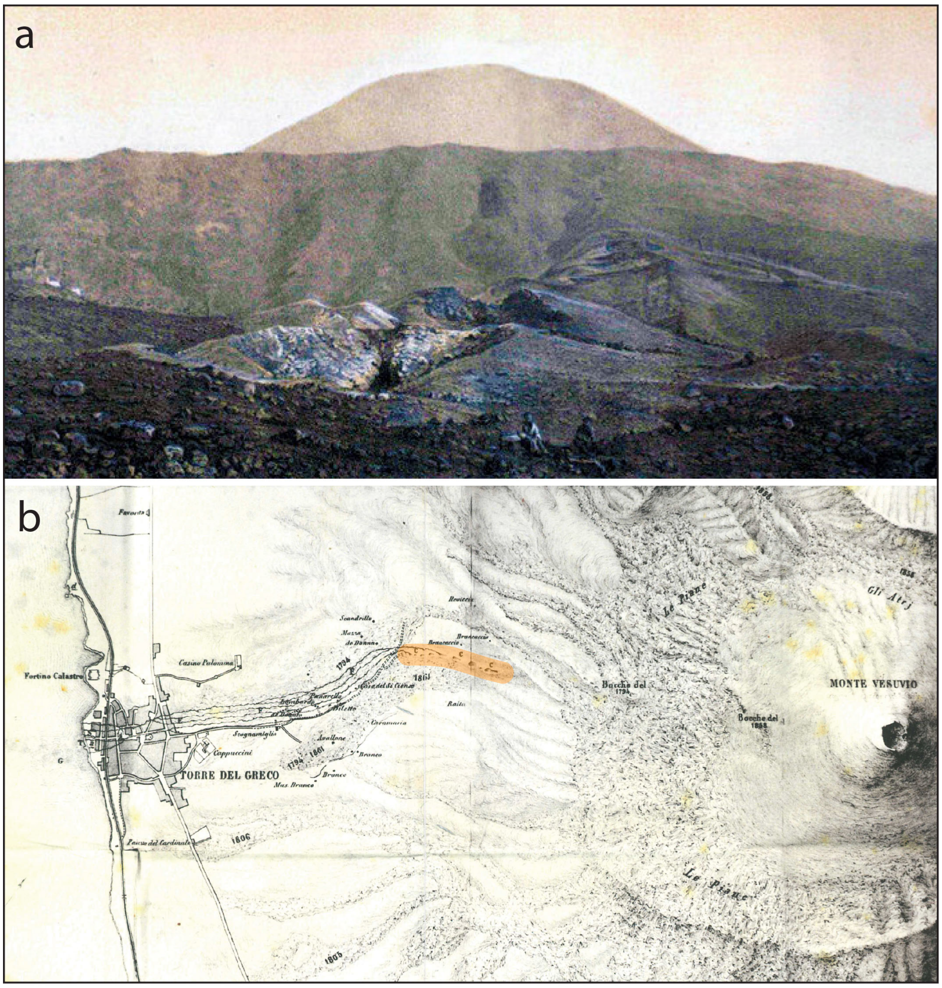

Figure 7. Vents and eruptive fissure of the 1861 eruption. (**a**) Photograph of the 1861 eruptive fissure and vents taken immediately after the eruption. In the foreground, there are the vents aligned on the N070° fissure. In the center, there is the *Pomici di Avellino* tuff cone. In the background, there is the *Gran Cono Vesuviano* (photograph by [73]). (**b**) Map from [73] showing the fracturing pattern of the 1861 eruption, including an N040°–050° fracture set without any lava discharge and the N070° eruptive fissure (highlighted in yellow) from which a short lava flow was emitted.

Figure 8. *Cont.*

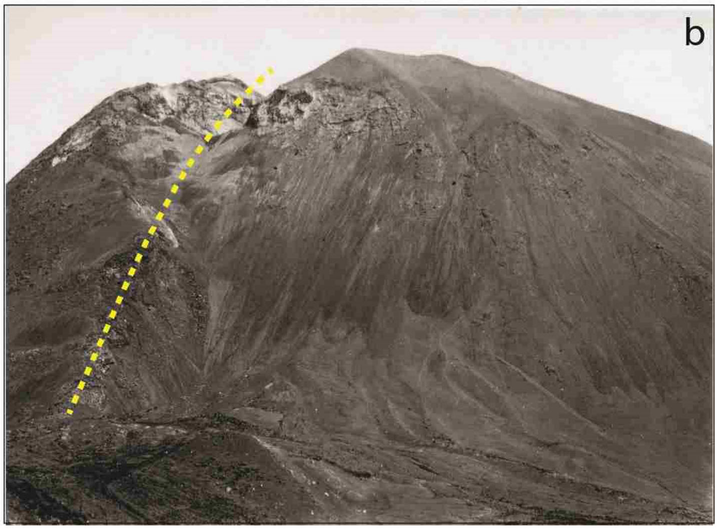

Figure 8. Vents and eruptive fissure of the 1872 eruption. (**a**) Photograph of the *Gran Cono Vesuviano* taken from the Vesuvio Observatory on 16 April 1872, before the start of the eruption. The yellow circle encloses a degassing parasitic cone nested on the crater rim (photo by Giorgio Sommer, 1872, printed by Giacomo Brogi, in Naples). (**b**) Post-eruption picture showing the eruptive fracture (dashed yellow line) oriented N320° and cutting all of the main Vesuvio cone, from the basal portion from which lava outpoured, forming an alignment of parasitic vents (photo by Giorgio Sommer, 1872, courtesy by Vincenzo Marasco).

6. Discussion

Here below, the results described in the previous chapter are summarized and discussed considering separately each synthem or sub-synthem. The reason for this approach will be apparent at the end of this section.

To characterize all of the structural patterns that acted within the Monte Somma and Vesuvio volcanic complex in the last 5600 years, it is advisable to briefly consider also vents, eruptive fissures, and structural elements linked to the previous *Somma* Super-Synthem. The vents lying on Monte Somma slopes (Case Sorrentino, Trapolino quarry, Pollena quarry, and Vallone San Severino) opened on weakness elements that follow the N040°–055° regional tectonic trend. Their stratigraphic position is between the deposits of *Pomici di Base* and Greenish Pumices which erupted 22,000 a BP and 19,200 a BP, respectively [3]. This implies that this tectonic trend was already active during this time interval. The north-eastern portion of the Monte Somma is characterized by a cliff modeled by the N300°–320° trend and pre-existing fractures of N040°–055° direction (Figure 4). The intersection of these two tectonic trends created favorable conditions for the formation of the dykes feeding the spatters of the Punta del Nasone Subsynthem between 22,000 and 19,200 a BP (Figure 4c; Table 1). To sum up, the N040°–055° and N300°–320°regional tectonic trends were active and controlled magmatic activity during at least the *Somma* Super-Synthem.

The Camaldoli hill cone—dated between the Pomici di Avellino and Pompei eruptions—is located on a sector of the volcano dominated by the N300°–320° elements (N. 59 in Figure 5). The Civita di Pompei center (N. 167 in Figure 3), instead, is positioned in relation to one of the main structures shaping the volcano substrate, that is, a regional-sized normal fault, striking EW and dipping N, that was identified by gravity surveys [22] (Figure 1b).

During the Pre-Historic Vesuvius Synthem (4000 a BP–5600 a BP), the morphology (and possibly the position) of the *Pomici di Avellino* tuff cone (N. 57) has been modeled by the N300°–320° trend.

During the Proto Vesuvius Synthem (AD 79—4000 a BP), the N300°–320° trend controlled the location of the offshore volcanic vents (e.g., the Torre Bassano vents, N. 21 and N. 24), the formation of the Fosso della Vetrana faults, as well as the opening of the AP explosive vents.

As a matter of fact, in the literature preceding [15,17], only the Viulo and Fossa Monaca vents (No. 91 and 95, respectively, in Figure 3; Table 1) positioned on an NNE local structural trend were recognized under the Medieval Vesuvius Synthem (1139—AD 472). In contrast, we found that the N300°–320° trend combined with the N070° trend was active since after the AD 79 eruption. In fact, the medieval lava flows were channeled into the N070°-trending valleys produced by the erosion of the Pompei AD 79 eruption deposits [17] (Figure 2). Vent location confirms that even during medieval times, the main active trend was still the N300°–320°, as already found by [15,17]. The abundance of vents, mainly located inland but a few km from the coast, testifies an intense monogenetic activity unrelated with a central edifice which caused the emission of lava flows with the most primitive composition among Vesuvio products [75]. This kind of activity was not considered in predictive studies of future events that were focused on the hazard due to the explosive behavior of the volcano e.g., [76–78]. Our works show that this type of activity is more common at Vesuvius than previously thought.

For what concerns the vents identified in the last period of Vesuvio activity, that is, the Present Vesuvius Synthem (1944–1631), some have a location that shows a correlation with morpho-structural domains—as can be defined the Monte Somma caldera or the *Gran Cono Vesuviano* or the Monte Somma and Vesuvio slopes—whereas there is no correlation in other cases. In fact, relatively old vents (e.g., those associated with the 1751 eruption) opened on the AD 79 caldera floor, and relatively younger vents (e.g., 1872 and 1941) opened on the upper flanks of the main Vesuvio cone, while important vent clusters (such as the 1858 and 1906 ones) are distributed partly inside and partly outside the caldera rim. In particular, the 1906 vents are aligned along the N040°–055° regional tectonic trend rather than in a radial distribution on the main cone. This "disordered" behavior is indicative of strong control operated by deep-reaching tectonic trends on the opening location of the vents, demonstrating the nil to negligible importance of local factors, such as the increase in weight on the bottom of the caldera [79] induced by the accumulation of lava flows, or the structural barrier [45] generated in the SE portion of the volcano by the caldera fault linked to the AD 79 eruption (Figure 2).

For the Present Vesuvius Synthem, vent analysis has demonstrated that the N300°–320° Apennine tectonic trend was not so active in this period, in that few vents are positioned on structures directly relatable to this trend, such as the main 1872 fracture (Figure 8). Vents of the eruptions characterized by more than one eruptive fissure (e.g., 1858 and 1906) are frequently positioned on N040°–055° trend elements (Figure 4).

An NNW structural trend affected the easternmost sector of the Monte Somma cliff (Cognoli di Levante area) and the related portion of the caldera floor, as well as the south-eastern part of the AD 79 caldera rim, giving rise to a significant number of vents positioned outside the caldera domain in both the 19th and 20th centuries (Figures 3 and 4), the best known of which are the 1760 vents, known as "Le Voccole" (Figure 5). The regional EW tectonic trend, already identified into the Civita di Pompei area, emerges also from the rose diagram of the eruptive fissures that sliced the main Vesuvio cone, in addition to the other already mentioned trends [8–10] recognized an alleged radial trend for the eruptive fractures that opened on the main Vesuvio cone during the three and half centuries of generally considered open-conduit activity of the Present Vesuvius Synthem. However, there is no radial trend on the main Vesuvio cone, as shown by the analysis of both the 85 eruptive fissures from [45] and the 61 eruptive fissures reported by [46] (Figure 4b). In contrast, the analysis of [8] was performed on a selection of 37 fractures only. We reiterate that the main Vesuvio cone during the post-1631 eruptive period was intersected by prevalent NS and EW fracture trends, in addition to the N300°–320° and N040°–055° trends, in partial agreement with [11].

Our positioning in time and space of the numerous monogenetic vents that punctuated the Vesuvio activity during the last 5600 years has relevant implications in forecasting the location of the eruptive fissures and vents in case of future unrest of the volcano. In fact, this study demonstrates that fissure activity was not controlled only by a set of radial eruptive fissures on the central edifice (the Gran Cono Vesuviano), as previously thought. On the contrary, the considerable number of vents and related eruptive fissures show that effusive monogenetic activity was important at Vesuvio in the past. The opening and location of the vents were governed by the main regional tectonic trends, which activated from time to time. This fact suggests that regional or local tectonic stress will probably control the opening of eruptive fissures and vents in the future. In this study, we found that five tectonic trends acted as pathway of magma rise toward the surface during the life of the volcano and that two of these tectonic trends characterized the most recent monogenetic activity. Therefore, we can speculate that in the future, magma will rise and discharge through eruptive fissures related to N040°–055° regional elements possibly associated with the N300°–320° regional fractures. The resulting emission of rapidly moving lava flows might cause huge damage in such a densely populated volcanic area and might seriously affect the management of future emergencies, adding a further element of risk to those already foreseen in the case of explosive eruptions e.g., [76–78].

It should be noted that a distinct structural behavior of the volcano characterized each synthem or sub-synthem here defined. In addition, the space distribution of vents and eruptive fissures, as well as in general the eruptive style of the volcano, turns out, from this study, to be different for each different synthematic unit. Thus, these differences in structural behavior and volcanic activity coincide with the time windows defined by the adopted synthematic sub-division. This strict cause–effect link between regional tectonics and volcanic activity would have never been revealed without the adoption of stratigraphic units limited by unconformities. Once more, this unprecedented result for Vesuvio highlights the effectiveness of the UBSU approach in volcanology.

7. Conclusions

In this study, 168 monogenetic vents have been positioned in space and time and related to specific structural and volcano-tectonic features. We showed that (i) the opening and location of the vents were controlled by five regional tectonic trends which activated on Monte Somma and Vesuvio in different time intervals corresponding to the distinct synthematic units adopted, and that (ii) this type of activity was more important during the life of the volcano than previously thought.

The oldest period of volcanic activity of the Monte Somma and Vesuvio volcanic complex, between 39,000 and 5600 years ago, was dominated by the joint action of N300°–320° and N040°–055° regional trends. Volcanic quiescence started 5600 years ago, during the period characterized by the Versilian Marine Transgression that marks the boundary between the Somma Super-Synthem and the Vesuvius Super-Synthem. This stasis of volcanic activity was probably associated with a stop of regional tectonics. The recovery of volcanic activity occurred about 4000 years ago (Table 1), within an evidently different tectonic framework, characterized by the joint action of the N070° and EW regional trends with the two local-scale NNW and NNE trends, and the persistence of a high degree of fragility along the N300°–320° and N040°–055° previously active regional trends.

The combined action of all of the tectonic trends mentioned above has led to the creation of a high number of eruptive fissures and related monogenetic vents, distributed across the entire surface and throughout the whole life of the volcano. However, only the N040°–055° and the N300°–320° elements controlled the most recent monogenetic activity. Therefore, we suggest that in the future, magma will rise and discharge through eruptive fissures related to these two regional tectonic trends. Furthermore, it follows that the future expected eruption might occur not only from the central volcano, as considered so far, but also from an eruptive fissure opened on its slopes, resulting in the emission of rapidly moving lava flows in densely populated areas. In other words, this study adds a new risk scenario to those already established so far in case of medium-to-long-term unrest at Vesuvio volcano.

Author Contributions: Conceptualization, C.P., D.G. and A.P.; methodology, C.P. and A.P.; software, A.P.; investigation, C.P., D.B., S.A., A.P. and D.G.; data curation, C.P., S.A., D.B. and A.P.; writing—

original draft preparation, C.P.; writing—review and editing, C.P., A.P., D.G. and S.L.F. All authors have read and agreed to the published version of the manuscript.

Funding: The fieldwork was supported by partial funding of the Italian Department of Civil Protection and of Vesuvius National Park. D.G. and C.P. acknowledge the support from a CSIS-CNR (2011) bilateral project. D.G. also acknowledges the contribution to this research provided by the local research funds of 2011–2016 of the University of Turin. The publication fee of this article was supported by JRU EPOS Italia funding (S.L.F.).

Data Availability Statement: Data on vents are reposted in Appendix A; .jpgw files of digitized ancient chartography can be provided upon reasonable request to the Corresponding Author.

Acknowledgments: C.P. is indebted to Joan Hernandez, Luigina Vezzoli, and Emilio Casciello for fruitful discussions during field-work and encouragement to write this paper.

Conflicts of Interest: Author Debora Brocchini is employed by the company Parchi Val di Cornia. The remaining authors declare that the research was conducted in the absence of any commercial or financial relationship that could be construed as a potential conflict of interest.

Appendix A

Table A1. Collection of the Monte Somma and Vesuvio vents information.

Vents	X Coordinate	Y Coordinate	Typology	Super-Synthem	Synthem	Sub-Synthem	Name/Locality	Assigned Age	References
1	441678.8639	4512546.465	undersea cryptodome				Gulf of Naples	<19,000 y BP	Milia et al., 1998 [31]
2	442228.1	4512121.49	off-shore vent				Gulf of Naples	unknown	Finetti & Morelli 1974 [20]
3	442806.87	4511708.08	off-shore vent				Gulf of Naples	unknown	Finetti & Morelli 1974 [20]
4	443036.1791	4511263.233	undersea cryptodome				Gulf of Naples	<19,000 y BP	Milia et al., 1998 [31]
5	444094.5146	4511355.837	undersea cryptodome				Gulf of Naples	<19,000 y BP	Milia et al., 1998 [31]
6	444575.3957	4510142.72	undersea cryptodome				Gulf of Naples	<19,000 y BP	Milia et al., 1998 [31]
7	444646.5468	4512941.136	off-shore vent				Gulf of Naples	<19,000 y BP	Aiello et al., 2010 [32]; Paoletti et al., 2016 [33]
8	445003.735	4511978.051	off-shore vent				Gulf of Naples	<19,000 y BP	Aiello et al., 2010 [32]; Paoletti et al., 2016 [33]
9	445049	4514522.02	undersea pit crater				Gulf of Naples	unknown	Milia et al., 1998 [31]
10	445651.9655	4511358.925	off-shore vent				Gulf of Naples	<19,000 y BP	Paoletti et al., 2016 [33]
11	446168.871	4517267.602	inferred vent	Vesuvio	Medieval Vesuvius	Miglio d'Oro	Favorita	9th−10th century	Paolillo et al., 2016 [17]
12	446423.311	4524520.8	spatter cone	Proto Somma	Trapolino		Cercola/Masseria San Giovanni	39,000–22,000 y BP	Johnston-Lavis 1884 [57], this work
13	446627.7554	4509801.272	off-shore vent				Gulf of Naples	<19,000 y BP	Aiello et al., 2010 [32]; Paoletti et al., 2016 [33]
14	446928.46	4516303.66	spatter cone	Vesuvio	Medieval Vesuvius	Miglio d'Oro	Calastro	9th−10th century	Paolillo et al., 2016 [17]
15	447240.95	4517461.78	spatter cone	Vesuvio	Medieval Vesuvius	Miglio d'Oro	I Tironi	1006–07	Paolillo et al., 2016 [17]
16	447432.66	4517463.43	spatter cone	Vesuvio	Medieval Vesuvius	Miglio d'Oro	I Tironi	1006–07	Paolillo et al., 2016 [17]

Table A1. *Cont.*

Vents	X Coordinate	Y Coordinate	Typology	Super-Synthem	Synthem	Sub-Synthem	Name/Locality	Assigned Age	References
17	447610.26	4517160.78	inferred vent	Vesuvio	Medieval Vesuvius	Miglio d'Oro	I Tironi	1006–07	Paolillo et al., 2016 [17]
18	447662.73	4519361.85	lava cumulus	Vesuvio	Present Vesuvius	Piano delle Ginestre	Novelle di Scappa	1858	Paolillo et al., 2016 [17]
19	447666.21	4519677.42	lava cumulus	Vesuvio	Present Vesuvius	Piano delle Ginestre	Novelle di Scappa	1858	This work
20	447696.3	4518866.16	covered vent	Vesuvio	Medieval Vesuvius	Miglio d'Oro	Sotto i Troni/Novelle di San Vito	9th—10th century	Paolillo et al., 2016 [17]
21	447788.31	4513637.83	spatter cone	Vesuvio	Proto Vesuvius	Pre-Roman	Torre Bassano	AD 79–4000 y BP	Di Girolamo 1970 [54]; Paolillo et al., 2016 [17]
22	447805.1536	4511195.629	off-shore vent				Gulf of Naples	<19,000 y BP	Aiello et al., 2010 [32]; Paoletti et al., 2016 [33]
23	447834.3	4519030.09	lava cumulus	Vesuvio	Present Vesuvius	Piano delle Ginestre	Novelle di San Vito	1858	Paolillo et al., 2016 [17]
24	447835.73	4513580.94	spatter cone	Vesuvio	Proto Vesuvius	Pre-Roman	Torre Bassano	AD 79–4000 y BP	Di Girolamo 1970 [54]; Paolillo et al., 2016 [17]
25	447839.67	4520295.24	spatter cone	Proto Somma	Trapolino		Case Sorrentino	22,000–19,200 y BP	Brocchini 1999 [34]
26	447958.69	4519418.09	lava cumulus	Vesuvio	Present Vesuvius	Piano delle Ginestre	Novelle di Scappa	1858	This work
27	447990.16	4519194.7	lava cumulus	Vesuvio	Present Vesuvius	Piano delle Ginestre	Novelle di San Vito	1858	Paolillo et al., 2016 [17]
28	448138.58	4519206.52	lava cumulus	Vesuvio	Present Vesuvius	Piano delle Ginestre	Novelle di San Vito	1858	Paolillo et al., 2016 [17]
29	448202.95	4517736.81	spatter cone	Vesuvio	Present Vesuvius	Piano delle Ginestre	Montedoro	1794	Rosi et al., 1986 [2]; Paolillo et al., 2016 [17]
30	448209.42	4519052.94	lava cumulus	Vesuvio	Present Vesuvius	Piano delle Ginestre	Novelle di San Vito	1858	Paolillo et al., 2016 [17]
31	448266.51	4517219.6	spatter cone	Vesuvio	Present Vesuvius	Piano delle Ginestre	Montedoro	1861	Rosi et al., 1986 [2]; Paolillo et al., 2016 [17]

Table A1. *Cont.*

Vents	X Coordinate	Y Coordinate	Typology	Super-Synthem	Synthem	Sub-Synthem	Name/Locality	Assigned Age	References
32	448308.62	4517240.07	spatter cone	Vesuvio	Present Vesuvius	Piano delle Ginestre	Montedoro	1861	Rosi et al., 1986 [2]; Paolillo et al., 2016 [17]
33	448361.9	4517259.82	spatter cone	Vesuvio	Present Vesuvius	Piano delle Ginestre	Montedoro	1861	Rosi et al., 1986 [2]; Paolillo et al., 2016 [17]
34	448365.13	4514499.76	inferred vent	Vesuvio	Medieval Vesuvius	Miglio d'Oro	Torre Bassano/L'Epitaffio	968 BC	Paolillo et al., 2016 [17]
35	448393.14	4518889.7	lava cumulus	Vesuvio	Present Vesuvius	Piano delle Ginestre	Piano delle Ginestre	1858	Paolillo et al., 2016 [17]
36	448399.07	4517976.71	spatter cone	Vesuvio	Present Vesuvius	Piano delle Ginestre	Montedoro	1794	Rosi et al., 1986 [2]; Paolillo et al., 2016 [17]
37	448461.57	4518019.46	spatter cone	Vesuvio	Present Vesuvius	Piano delle Ginestre	Montedoro	1794	Rosi et al., 1986 [2]; Paolillo et al., 2016 [17]
38	448490.34	4517313.3	spatter cone	Vesuvio	Present Vesuvius	Piano delle Ginestre	Montedoro	1861	Rosi et al., 1986 [2]; Paolillo et al., 2016 [17]
39	448539.77	4518062.81	spatter cone	Vesuvio	Present Vesuvius	Piano delle Ginestre	Montedoro	1794	Rosi et al., 1986 [2]; Paolillo et al., 2016 [17]
40	448555.28	4517340.79	spatter cone	Vesuvio	Present Vesuvius	Piano delle Ginestre	Montedoro	1861	Rosi et al., 1986 [2]; Paolillo et al., 2016 [17]
41	448562.09	4518962.98	lava cumulus	Vesuvio	Present Vesuvius	Piano delle Ginestre	Piano delle Ginestre	1858	Paolillo et al., 2016 [17]
42	448566.83	4518075.91	spatter cone	Vesuvio	Present Vesuvius	Piano delle Ginestre	Montedoro	1794	Rosi et al., 1986 [2]; Paolillo et al., 2016 [17]
43	448627.82	4517396.22	spatter cone	Vesuvio	Present Vesuvius	Piano delle Ginestre	Montedoro	1861	Rosi et al., 1986 [2]; Paolillo et al., 2016 [17]
44	448706.49	4517448.91	spatter cone	Vesuvio	Present Vesuvius	Piano delle Ginestre	Montedoro	1861	Rosi et al., 1986 [2]; Paolillo et al., 2016 [17]
45	448724.33	4519353	lava cumulus	Vesuvio	Present Vesuvius	Piano delle Ginestre	Piano delle Ginestre	1858	Paolillo et al., 2016 [17]
46	448748.29	4519486.13	lava cumulus	Vesuvio	Present Vesuvius	Piano delle Ginestre	Piano delle Ginestre	1858	This work

Table A1. *Cont.*

Vents	X Coordinate	Y Coordinate	Typology	Super-Synthem	Synthem	Sub-Synthem	Name/Locality	Assigned Age	References
47	448780.85	4517494.39	spatter cone	Vesuvio	Present Vesuvius	Piano delle Ginestre	Montedoro	1861	Rosi et al., 1986 [2]; Paolillo et al., 2016 [17]
48	448813.74	4519405.35	lava cumulus	Vesuvio	Present Vesuvius	Piano delle Ginestre	Piano delle Ginestre	1858	This work
49	448948.89	4521815.89	spatter cone	Somma	Cognoli di Ottaviano	Canale dell'Arena	Pollena Quarry	22,000–19,200 y BP	Rosi et al., 1986 [2]; this work
50	449012.39	4521752.39	spatter cone	Proto Somma	Trapolino		Pollena Quarry	39,000–22,000 y BP	Rosi et al., 1986 [2]; this work
51	449162.87	4518099.51	spatter cone	Vesuvio	Present Vesuvius	Piano delle Ginestre	Piano delle Ginestre	1794	Rosi et al., 1986 [2]; Paolillo et al., 2016 [17]
52	449225.22	4518134.47	spatter cone	Vesuvio	Present Vesuvius	Piano delle Ginestre	Piano delle Ginestre	1794	Rosi et al., 1986 [2]; Paolillo et al., 2016 [17]
53	449247.07	4519178.75	covered vent	Vesuvio	Present Vesuvius	Piano delle Ginestre	Piano delle Ginestre	1858	Paolillo et al., 2016 [17]
54	449253.69	4519308.21	lava cumulus	Vesuvio	Present Vesuvius	Piano delle Ginestre	Piano delle Ginestre	1858	Paolillo et al., 2016 [17]
55	449349.48	4518156.97	covered vent	Vesuvio	Present Vesuvius	Piano delle Ginestre	Piano delle Ginestre	1794	Rosi et al., 1986 [2]; Paolillo et al., 2016 [17]
56	449462.52	4519511.37	covered vent	Vesuvio	Present Vesuvius	Piano delle Ginestre	Piano delle Ginestre	1858	Allievi 1875 (Tav.5) [40]; this work
57	449492.31	4518683.72	central vent	Vesuvio	Proto Vesuvius	Avellino	Avellino tuff-cone/Piano delle Ginestre	4000 y BP	Principe et al., 2021 [56]
58	449599.9	4518232.51	spatter cone	Vesuvio	Present Vesuvius	Piano delle Ginestre	Piano delle Ginestre	1794	Rosi et al., 1986 [2]; Paolillo et al., 2016 [17]
59	449817	4514547.44	cinder cone	Vesuvio	Proto Vesuvius	Pre-Roman	Camaldoli della Torre	AD 79–4000 y BP	Rosi et al., 1986 [2]; Paolillo et al., 2016 [17]
60	450010.59	4518508.78	lava cumulus	Vesuvio	Present Vesuvius	Piano delle Ginestre	Piano delle Ginestre	1858	Paolillo et al., 2016 [17]

Table A1. *Cont.*

Vents	X Coordinate	Y Coordinate	Typology	Super-Synthem	Synthem	Sub-Synthem	Name/Locality	Assigned Age	References
61	450075.8	4518642.97	lava cumulus	Vesuvio	Present Vesuvius	Piano delle Ginestre	Piano delle Ginestre	1858	Paolillo et al., 2016 [17]
62	450140.05	4518492.72	lava cumulus	Vesuvio	Present Vesuvius	Piano delle Ginestre	Piano delle Ginestre	1858	Paolillo et al., 2016 [17]
63	450285.57	4518744.08	covered vent	Vesuvio	Present Vesuvius	Piano delle Ginestre	Piano delle Ginestre	1858	Paolillo et al., 2016 [17]
64	450388.08	4519188.24	lava cumulus	Vesuvio	Present Vesuvius	Piano delle Ginestre	Gran Cono	1858	Paolillo et al., 2016 [17]
65	450398.35	4519277.82	covered vent	Vesuvio	Present Vesuvius	Piano delle Ginestre	Gran Cono	1858	Allievi 1875 (Tav.4) [40]; this work
66	450457.89	4519751.32	lava cumulus	Vesuvio	Present Vesuvius	Piano delle Ginestre	Colle Umberto	1895–99	Rosi et al., 1986 [2]; this work
67	450472.17	4519227.02	covered vent	Vesuvio	Present Vesuvius	Piano delle Ginestre	Gran Cono	1858	Allievi 1875 (Tav.4) [40]; this work
68	450593.61	4519284.17	covered vent	Vesuvio	Present Vesuvius	Piano delle Ginestre	Gran Cono	1858	Allievi 1875 (Tav.4) [40]; this work
69	450669.22	4518904.72	covered vent	Vesuvio	Present Vesuvius	Piano delle Ginestre	Gran Cono	1858	Allievi 1875 (Tav.4) [40]; this work
70	450719.33	4519968.37	central vent	Proto Somma	Cognoli di Trocchia		Trocchia volcano/Atrio del Cavallo	39,000–22,000 y BP	Principe et al., 2021 [56]
71	450806.2	4519712.08	covered vent	Vesuvio	Present Vesuvius	Piano delle Ginestre	Bocca di Countrel	1820	Allievi 1875 (Tav.4) [40]; this work
72	450932.31	4516471	cinder cone	Vesuvio	Medieval Vesuvius	Miglio d'Oro	Montagnelle/ Monticelli	999 AD	Allievi 1875 (Tav.4) [40]; Rosi et al., 1986 [2]; Principe et al., 2004 [15]; this work
73	451040.87	4516393.72	covered vent	Vesuvio	Medieval Vesuvius	Miglio d'Oro	Montagnelle/ Monticelli	999 AD	Rosi et al., 1986 [2]; Principe et al., 2004 [15]; this work

Table A1. *Cont.*

Vents	X Coordinate	Y Coordinate	Typology	Super-Synthem	Synthem	Sub-Synthem	Name/Locality	Assigned Age	References
74	451137.29	4516306.2	covered vent	Vesuvio	Medieval Vesuvius	Miglio d'Oro	Montagnelle/ Monticelli	999 AD	Rosi et al., 1986 [2]; Principe et al., 2004 [15]; this work
75	451327.88	4519760.2	spatter cone	Vesuvio	Present Vesuvius	Piano delle Ginestre	Gran Cono	1872	This work
76	451389.6	4519652.31	spatter cone	Vesuvio	Present Vesuvius	Piano delle Ginestre	Gran Cono	1941	This work
77	451510.97	4518315.55	covered vent	Vesuvio	Present Vesuvius	Piano delle Ginestre	Gran Cono	1737	Allievi 1875 (Tav.5) [40]; this work
78	451548	4519743.74	covered vent	Vesuvio	Present Vesuvius	Piano delle Ginestre	Gran Cono	1872	Allievi 1875 (Tav.5) [40]; this work
79	451554.02	4520003.01	lava cumulus	Vesuvio	Present Vesuvius	Piano delle Ginestre	Colle Margherita	1891–94	Fiechter 1906 [43]; Rosi et al., 1986 [2]; this work
80	451606.88	4519075.37	central vent	Vesuvio	Present Vesuvius	Piano delle Ginestre	Gran Cratere	1944	Rosi et al., 1986 [2]; this work
81	451618.86	4520141.62	central vent	Somma	Cognoli di Ottaviano	Canale dell'Arena	Arena volcano/Valle del Gigante	22,000–19,200 y BP	Principe et al., 2021 [56]
82	451618.89	4520053.17	lava cumulus	Vesuvio	Present Vesuvius	Piano delle Ginestre	Colle Margherita	1891–94	Fiechter 1906 [43]; Rosi et al., 1986 [2]; this work
83	451675.04	4515698.51	spatter cone	Vesuvio	Present Vesuvius	Piano delle Ginestre	Le Voccole	1760	Allievi 1875 (Tav.5) [40]; Rosi et al., 1986 [2]; this work
84	451692.9346	4520819.426	welded spatter	Somma	Cognoli di Ottaviano	Punta del Nasone	Punta del Nasone	19,200–8900 y BP	Brocchini 1999 [34]; this work
85	451693.41	4515540.22	spatter cone	Vesuvio	Present Vesuvius	Piano delle Ginestre	Le Voccole	1760	Allievi 1875 (Tav.5) [40]; this work
86	451694.2	4515465.61	spatter cone	Vesuvio	Present Vesuvius	Piano delle Ginestre	Le Voccole	1760	Allievi 1875 (Tav.5) [40]; this work
87	451695.94	4519203.7	central vent	Vesuvio	Present Vesuvius	Piano delle Ginestre	Gran Cratere	1872	Allievi 1875 (Tav.5) [40]

Table A1. *Cont.*

Vents	X Coordinate	Y Coordinate	Typology	Super-Synthem	Synthem	Sub-Synthem	Name/Locality	Assigned Age	References
88	451710.76	4515347.31	spatter cone	Vesuvio	Present Vesuvius	Piano delle Ginestre	Le Voccole	1760	Allievi 1875 (Tav.6) [40]; Rosi et al., 1986 [2]; this work
89	451743.25	4519196.94	central vent	Vesuvio	Present Vesuvius	Piano delle Ginestre	Gran Cratere	1906	Fiechter 1906 [43]
90	451769.159	4520865.885	welded spatter	Somma	Cognoli di Ottaviano	Punta del Nasone	Punta del Nasone	19,200–8900 y BP	Brocchini 1999 [34]; this work
91	451853.9649	4513973.256	spatter cone	Vesuvio	Medieval Vesuvius	Miglio d'Oro	Viulo	991 AD	Allievi 1875 (Tav.6) [40]; Rosi et al., 1986 [2]; Principe et al. 2004 [15]; this work
92	451873.24	4517959.91	spatter cone	Vesuvio	Present Vesuvius	Piano delle Ginestre	Gran Cono	1906	This work
93	451892.74	4519615.6	covered vent	Vesuvio	Present Vesuvius	Piano delle Ginestre	Gran Cono	1834	Fiechter 1904 [42]; this work
94	451898.64	4518052.78	spatter cone	Vesuvio	Present Vesuvius	Piano delle Ginestre	Gran Cono	1906	This work
95	451919.55	4514262.26	spatter cone	Vesuvio	Medieval Vesuvius	Miglio d'Oro	Fossa Monaca	991 AD	Allievi 1875 (Tav.6) [40]; Rosi et al., 1986 [2]; Principe et al., 2004 [15]; this work
96	451927.51	4519900.45	covered vent	Vesuvio	Present Vesuvius	Piano delle Ginestre	Gran Cono	1834	Allievi 1875 (Tav.5) [40]; this work
97	451939.12	4518063.1	spatter cone	Vesuvio	Present Vesuvius	Piano delle Ginestre	Gran Cono	1906	Fiechter 1904 [42]; this work
98	451945.65	4520154.49	covered vent	Vesuvio	Present Vesuvius	Piano delle Ginestre	Atrio del Cavallo	1834	Allievi 1875 (Tav.5) [40]; this work
99	451953.35	4519673.79	covered vent	Vesuvio	Present Vesuvius	Piano delle Ginestre	Gran Cono	1834	Fiechter 1904 [42]
100	451996.99	4519721.07	covered vent	Vesuvio	Present Vesuvius	Piano delle Ginestre	Gran Cono	1834	Allievi 1875 (Tav.5) [40]; this work

Table A1. *Cont.*

Vents	X Coordinate	Y Coordinate	Typology	Super-Synthem	Synthem	Sub-Synthem	Name/Locality	Assigned Age	References
101	452014.83	4519840.13	covered vent	Vesuvio	Present Vesuvius	Piano delle Ginestre	Atrio del Cavallo	1834	Allievi 1875 (Tav.5) [40]
102	452044.29	4517811.08	spatter cone	Vesuvio	Present Vesuvius	Piano delle Ginestre	Gran Cono	1906	This work,
103	452065.34	4517788.19	spatter cone	Vesuvio	Present Vesuvius	Piano delle Ginestre	Gran Cono	1906	This work
104	452073.56	4520040.95	covered vent	Vesuvio	Present Vesuvius	Piano delle Ginestre	Atrio del Cavallo	1834	Allievi 1875 (Tav.5) [40]; this work
105	452093.92	4517742.55	spatter cone	Vesuvio	Present Vesuvius	Piano delle Ginestre	Gran Cono	1906	This work
106	452152.03	4518254.97	covered vent	Vesuvio	Present Vesuvius	Piano delle Ginestre	Gran Cono	1754	Allievi 1875 (Tav.5) [40]; this work
107	452250.67	4517885.3	spatter cone	Vesuvio	Present Vesuvius	Piano delle Ginestre	Gran Cono	1906	This work
108	452265.63	4518163.64	covered vent	Vesuvio	Present Vesuvius	Piano delle Ginestre	Gran Cono	1754	Allievi 1875 (Tav.5 [40]); this work
109	452301.67	4518718.28	covered vent	Vesuvio	Present Vesuvius	Piano delle Ginestre	Gran Cono	1754	Allievi 1875 (Tav.5) [40]; this work
110	452343.02	4518032.8	spatter cone	Vesuvio	Present Vesuvius	Piano delle Ginestre	Gran Cono	1906	This work
111	452379.01	4518300.03	covered vent	Vesuvio	Present Vesuvius	Piano delle Ginestre	Gran Cono	1754	Allievi 1875 (Tav.5) [40]; this work
112	452396.87	4518111.78	spatter cone	Vesuvio	Present Vesuvius	Piano delle Ginestre	Gran Cono	1906	This work
113	452401.1	4518017.59	spatter cone	Vesuvio	Present Vesuvius	Piano delle Ginestre	Gran Cono	1906	This work
114	452418.66	4518959.87	spatter cone	Vesuvio	Present Vesuvius	Piano delle Ginestre	Gran Cono	unknown	This work
115	452450.7627	4520781.245	welded spatter	Somma	Cognoli di Ottaviano	Punta del Nasone	Cognoli di Ottaviano	19,200–8900 y BP	Brocchini 1999 [34]; this work

Table A1. *Cont.*

Vents	X Coordinate	Y Coordinate	Typology	Super-Synthem	Synthem	Sub-Synthem	Name/Locality	Assigned Age	References
116	452453.5906	4513203.357	inferred vent	Vesuvio	Medieval Vesuvius	Miglio d'Oro	Torre Annunziata/Case Cirillo	10th century	Principe et al., 2004 [15]; this work
117	452512.62	4518639.63	covered vent	Vesuvio	Present Vesuvius	Piano delle Ginestre	Gran Cono	1754	Allievi 1875 (Tav.5) [40]; this work
118	452530.35	4518448.99	covered vent	Vesuvio	Present Vesuvius	Piano delle Ginestre	Gran Cono	1906	This work
119	452531.6	4519088.27	covered vent	Vesuvio	Present Vesuvius	Piano delle Ginestre	Gran Cono	1882	Fiechter 1904 [42]; this work
120	452546.03	4519360.15	spatter cone	Vesuvio	Present Vesuvius	Piano delle Ginestre	Gran Cono	1903–04	Fiechter 1906 [43]; this work
121	452546.23	4518575.33	spatter cone	Vesuvio	Present Vesuvius	Piano delle Ginestre	Gran Cono	1906	This work
122	452554.16	4518510.51	spatter cone	Vesuvio	Present Vesuvius	Piano delle Ginestre	Gran Cono	1906	This work
123	452575.86	4518363.53	spatter cone	Vesuvio	Present Vesuvius	Piano delle Ginestre	Gran Cono	1850	Fiechter 1904 [42]; this work
124	452578.24	4518845.72	covered vent	Vesuvio	Present Vesuvius	Piano delle Ginestre	Gran Cono	1754	Allievi 1875 (Tav.5) [40]; this work
125	452587.63	4519466.57	spatter cone	Vesuvio	Present Vesuvius	Piano delle Ginestre	Gran Cono	1882	Fiechter 1904 [42]; this work
126	452595.36	4518441.99	spatter cone	Vesuvio	Present Vesuvius	Piano delle Ginestre	Vesuvius cone	1906	Fiechter 1906 [43]; this work
127	452632.42	4520567.05	welded spatter	Somma	Cognoli di Ottaviano	Punta del Nasone	Cognoli di Ottaviano	19,200–8900 y BP	Brocchini 1999 [34]; this work
128	452635.32	4518471.79	spatter cone	Vesuvio	Present Vesuvius	Piano delle Ginestre	Vesuvius cone	1906	Fiechter 1906 [43]; this work
129	452638.2701	4515223.323	spatter cone	Vesuvio	Medieval Vesuvius	Miglio d'Oro	Masseria Angeloni	Middle Age	This work

Table A1. *Cont.*

Vents	X Coordinate	Y Coordinate	Typology	Super-Synthem	Synthem	Sub-Synthem	Name/Locality	Assigned Age	References
130	452661.36	4518504.78	spatter cone	Vesuvio	Present Vesuvius	Piano delle Ginestre	Vesuvius cone	1906	Fiechter 1906 [43]; this work
131	452664.55	4518179.71	covered vent	Vesuvio	Present Vesuvius	Piano delle Ginestre	Valle dell'Inferno	1751	Allievi 1875 (Tav.5) [40]; this work
132	452676.27	4518523.92	spatter cone	Vesuvio	Present Vesuvius	Piano delle Ginestre	Vesuvius cone	1906	Fiechter 1906 [43]; this work
133	452687.16	4518944.73	central vent	Somma	Levante	Cognoli di Levante	Levante volcano/Valle dell'Inferno	8900–5600 y BP	Principe et al., 2021 [56]
134	452691.18	4518191.19	covered vent	Vesuvio	Present Vesuvius	Piano delle Ginestre	Valle dell'Inferno	1751	Allievi 1875 (Tav.5) [40]; this work
135	452702.34	4518536.73	spatter cone	Vesuvio	Present Vesuvius	Piano delle Ginestre	Valle dell'Inferno	1906	Fiechter 1906 [43]; this work
136	452717.41	4518461.42	spatter cone	Vesuvio	Present Vesuvius	Piano delle Ginestre	Gran Cono	1850	Fiechter 1904 [42]; this work
137	452717.84	4518371.32	covered vent	Vesuvio	Present Vesuvius	Piano delle Ginestre	Valle dell'Inferno	1751	Allievi 1875 (Tav.5) [40]; this work
138	452720.61	4518227.26	covered vent	Vesuvio	Present Vesuvius	Piano delle Ginestre	Valle dell'Inferno	1751	Allievi 1875 (Tav.5) [40]; this work
139	452735.3	4518386.14	covered vent	Vesuvio	Present Vesuvius	Piano delle Ginestre	Valle dell'Inferno	1751	Allievi 1875 (Tav.5) [40]; this work
140	452755.94	4518393.02	covered vent	Vesuvio	Present Vesuvius	Piano delle Ginestre	Valle dell'Inferno	1751	Allievi 1875 (Tav.5) [40]; this work
141	452773.19	4518573.99	spatter cone	Vesuvio	Present Vesuvius	Piano delle Ginestre	Valle dell'Inferno	1906	Fiechter 1906 [43]; this work
142	452784.56	4518242.52	covered vent	Vesuvio	Present Vesuvius	Piano delle Ginestre	Valle dell'Inferno	1751	Allievi 1875 (Tav.5) [40]; this work
143	452824.82	4518291.82	covered vent	Vesuvio	Present Vesuvius	Piano delle Ginestre	Valle dell'Inferno	1751	Allievi 1875 (Tav.5) [40]; this work

Table A1. *Cont.*

Vents	X Coordinate	Y Coordinate	Typology	Super-Synthem	Synthem	Sub-Synthem	Name/Locality	Assigned Age	References
144	452863.65	4518262.27	covered vent	Vesuvio	Present Vesuvius	Piano delle Ginestre	Valle dell'Inferno	1751	Allievi 1875 (Tav.5) [40]; this work
145	452886.95	4520218.33	welded spatter	Somma	Cognoli di Ottaviano	Punta del Nasone	Cognoli di Levante	19,200–8900 y BP	Brocchini 1999 [34]; this work
146	452917.06	4518263.32	covered vent	Vesuvio	Present Vesuvius	Piano delle Ginestre	Valle dell'Inferno	1751	Allievi 1875 (Tav.5) [40]; this work
147	452943.97	4518287.51	covered vent	Vesuvio	Present Vesuvius	Piano delle Ginestre	Valle dell'Inferno	1751	Allievi 1875 (Tav.5) [40]; this work
148	452981.15	4520884.55	inferred vent	Somma	Cognoli di Ottaviano	Canale dell'Arena	Vallone San Severino	22,000–19,200 y BP	Johnston-Lavis (1884 and 1891b) [57,58]; this work
149	453003.36	4518773.89	spatter cone	Vesuvio	Present Vesuvius	Piano delle Ginestre	Valle dell'Inferno	1906	Fiechter 1906 [43]
150	453026.53	4518759.43	spatter cone	Vesuvio	Present Vesuvius	Piano delle Ginestre	Valle dell'Inferno	1906	Fiechter 1906 [43]
151	453060.16	4519206.1	spatter cone	Vesuvio	Present Vesuvius	Piano delle Ginestre	Valle dell'Inferno	1882	Fiechter 1904 [42]; this work
152	453071.1	4520003.49	welded spatter	Somma	Cognoli di Ottaviano	Punta del Nasone	Cognoli di Levante	19,200–8900 y BP	Brocchini 1999 [34]; this work
153	453117.8	4518094.4	spatter cone	Vesuvio	Present Vesuvius	Piano delle Ginestre	Cognoli	1751	Fiechter 1904 [42]; this work
154	453181.87	4518794.41	spatter cone	Vesuvio	Present Vesuvius	Piano delle Ginestre	Valle dell'Inferno	1937	This work
155	453189.37	4518461.51	spatter cone	Vesuvio	Present Vesuvius	Piano delle Ginestre	Valle dell'Inferno	1883	Fiechter 1904 [42]; this work
156	453196.64	4518505.83	spatter cone	Vesuvio	Present Vesuvius	Piano delle Ginestre	Valle dell'Inferno	1883	Fiechter 1904 [42]; this work
157	453258.72	4518547.51	spatter cone	Vesuvio	Present Vesuvius	Piano delle Ginestre	Valle dell'Inferno	1883	Fiechter 1904 [42]; this work

Table A1. *Cont.*

Vents	X Coordinate	Y Coordinate	Typology	Super-Synthem	Synthem	Sub-Synthem	Name/Locality	Assigned Age	References
158	453261.25	4519101.32	spatter cone	Vesuvio	Present Vesuvius	Piano delle Ginestre	Valle dell'Inferno	1882	Fiechter 1904 [42]; this work
159	453262.91	4517745.36	spatter cone	Vesuvio	Present Vesuvius	Piano delle Ginestre	Cognoletto	1906	Fiechter 1906 [43]; Rosi et al., 1986 [2]; this work
160	453499.73	4521276.14	spatter cone	Proto Somma	Trapolino		Vallone San Severino	39,000–22,000 y BP	Johnston-Lavis (1884 and 1891b) [57,58]; Santacroce & Sbrana (2003) [3]
161	453506.3133	4513247.015	spatter cone	Vesuvio	Medieval Vesuvius	Miglio d'Oro	Masseria Bosco del Monaco	10th century	Principe et al., 2004 [15]
162	453669.06	4521456.05	spatter cone	Proto Somma	Trapolino		Vallone San Severino	39,000–22,000 y BP	Johnston-Lavis (1884 and 1891b) [57,58]; Santacroce & Sbrana (2003) [3]
163	453817.23	4521593.64	spatter cone	Proto Somma	Trapolino		Vallone San Severino	39,000–22,000 y BP	Johnston-Lavis (1884 and 1891b) [57,58]; Santacroce & Sbrana (2003) [3]
164	454060.65	4521752.39	spatter cone	Proto Somma	Trapolino		Vallone San Severino	39,000–22,000 y BP	Johnston-Lavis (1884 and 1891b) [57,58]; Santacroce & Sbrana (2003) [3]
165	454124.15	4521995.8	spatter cone	Proto Somma	Trapolino		Trapolino quarry	39,000–22,000 y BP	Rosi et al., 1986 [2]; this work
166	454452.23	4521953.47	spatter cone	Proto Somma	Trapolino		Vallone San Severino	39,000–22,000 y BP	Johnston-Lavis (1884 and 1891b) [57,58]; Santacroce & Sbrana (2003) [3]
167	456304.1152	4511473.239	cinder cone	Vesuvio	Proto Vesuvius	Pre-Roman	Pompei volcano/Civita di Pompei	AD 79–4000 y BP	Cinque & Irollo 2004 [49], this work
168	458207.8762	4522660.428	spatter cone	unknown	unknown		Strocchioni	unknown	Rosi et al. 1986 [2]

References

1. Santacroce, R. (Ed.) *Somma-Vesuvius*; Quaderni de 'La Ricerca Scientifica' CNR: Rome, Italy, 1986; Volume 114.
2. Rosi, M.; Santacroce, R.; Sbrana, A. Geological map of Somma-Vesuvius volcanic complex (scale 1,25,000). In *Somma-Vesuvius*; Santacroce, R., Ed.; Quaderni de 'La Ricerca Scientifica' CNR: Rome, Italy, 1986; Volume 114.
3. Santacroce, R.; Sbrana, A. *Carta Geologica del Vesuvio, Scala 1:15,000. Progetto CARG*; Servizio Geologico Nazionale-Consiglio Nazionale delle Ricerche: Firenze, Italy, 2003.
4. AQUATER. Rilievo Geologico-Vulcanologico area permesso Ottaviano, contratto n.532882. Relazione Finale, San Lorenzo in Campo, GEOS A0298. 1979.
5. Ventura, G.; Vilardo, G.; Bruno, P.P. The role of flank failure in modifying the shallow plumbing system of volcanoes: An example from Somma-Vesuvius, Italy. *Geophys. Res. Lett.* **1999**, *26*, 3681–3684. [CrossRef]
6. Cigolini, C.; Salierno, F.; Gervino, G.; Bergese, P.; Marino, C.; Russo, M.; Prati, P.; Ariola, V.; Bonetti, R.; Begnini, S. High-Resolution Radon Monitoring and Hydrodynamics at Mount Vesuvius. *Geophys. Res. Lett.* **2001**, *28*, 4035–4038. [CrossRef]
7. Sbrana, A.; Cioni, R.; Marianelli, P.; Sulpizio, R.; Andronico, D.; Pasquini, G. Volcanic evolution of the Somma-Vesuvius Complex (Italy). *J. Maps* **2020**, *16*, 137–147. [CrossRef]
8. Acocella, V.; Porreca, M.; Neri, M.; Massimi, E.; Mattei, M. Propagation of dikes at Vesuvio (Italy) and the effect on Mt. Somma. *Geophys. Res. Lett.* **2006**, *33*, L08301. [CrossRef]
9. Acocella, V.; Porreca, M.; Neri, M.; Mattei, M.; Funiciello, R. Fissure eruptions at Mount Vesuvius (Italy): Insights on the shallow propagation of dikes at volcanoes. *Geology* **2006**, *34*, 673–676. [CrossRef]
10. Porreca, M.; Acocella, V.; Massimi, E.; Mattei, M.; Funiciello, R.; De Benedetti, A.A. Geometric and kinematic features of the dike complex at Mt. Somma, Vesuvio (Italy). *Earth Planet. Sci. Lett.* **2006**, *245*, 389–407. [CrossRef]
11. Tramparulo, F.D.A.; Vitale, S.; Isaia, R.; Tadini, A.; Bisson, M.; Prinzi, E.P. Relation between alternating open/closed-conduit conditions and deformation patterns: An example from the Somma-Vesuvius volcano (southern Italy). *J. Struct. Geol.* **2018**, *112*, 138–153. [CrossRef]
12. Cioni, R.; Santacroce, R.; Sbrana, A. Pyroclastic deposits as a guide for reconstructing e multi-stage evolution of the Somma-Vesuvius caldera. *Bull. Volcanol.* **1999**, *61*, 207–222. [CrossRef]
13. Tadini, A.; Bisson, M.; Neri, A.; Cioni, R.; Bevilacqua, A.; Aspinall, W.P. Assessing future vent opening locations at the Somma-Vesuvio volcanic complex: 1. A new information geo-database with uncertainty characterizations: A geo-database for Somma-Vesuvio. *J. Geophys. Res. Solid Earth* **2018**, *122*, 4336–4356. [CrossRef]
14. Tadini, A.; Bevilacqua, A.; Neri, A.; Cioni, R.; Aspinall, W.P.; Bisson, M.; Isaia, R.; Mazzarini, F.; Valentine, G.A.; Vitale, S.; et al. Assessing future vent opening locations at the Somma-Vesuvio volcanic complex: 2. Probability maps of the caldera for a future Plinian/sub-Plinian event with uncertainty quantification: Vent Opening Probability map for Vesuvio. *J. Geophys. Res. Solid Earth* **2018**, *122*, 4357–4376. [CrossRef]
15. Principe, C.; Tanguy, J.C.; Arrighi, S.; Paiotti, A.; Le Goff, M.; Zoppi, U. Chronology of Vesuvius' activity from AD 79 to 1631 based on archeomagnetism of lava flows and historical sources. *Bull. Volcanol.* **2004**, *66*, 703–724. [CrossRef]
16. Principe, C.; Brocchini, D.; Arrighi, S.; Luongo, G.; Giordano, D.; Perillo, M.; Di Muro, A.; Martì, J.M.; Bisson, M.; Paolillo, A. *Vesuvius Volcano-Tectonic History—A New Perspective*; IAVCEI Collapse Caldera Commission Workshop: Rome, Italy, 2010; pp. 51–53.
17. Paolillo, A.; Principe, C.; Bisson, M.; Gianardi, R.; Giordano, D.; La Felice, S. Volcanology of the South-Western sector of Vesuvius, Italy. *J. Maps* **2016**, *12*, 425–440. [CrossRef]
18. Arnò, V.; Principe, C.; Rosi, M.; Santacroce, R.; Sbrana, A.; Sheridan, M.F. Chapter 2. Eruptive history. In *Somma-Vesuvius*; Santacroce, R., Ed.; Quaderni de 'La Ricerca Scientifica' CNR: Rome, Italy, 1987; Volume 114, pp. 53–103.
19. Salvador, A. Unconformity-bounded stratigraphic units. *Geol. Soc. Am. Bull.* **1987**, *98*, 232–237.
20. Finetti, I.; Morelli, C. Esplorazione sismica a riflessione dei Golfi di Napoli e Pozzuoli. *Boll. Geofis. Teor. Appl.* **1974**, *XVI*, 175–222.
21. La Torre, P.; Nannini, R.; Sbrana, A. Geothermal exploration in Southern Italy: Geophysical interpretation of the Vesuvian area. *Boll. Geofis. Teor. Ed Appl.* **1983**, *26* (Suppl. 130), 197–208.
22. Cassano, E.; La Torre, P. Chapter 4. Geophysics. In *Somma-Vesuvius*; Santacroce, R., Ed.; Quaderni de 'La Ricerca Scientifica' CNR: Rome, Italy, 1987; Volume 114, pp. 175–196.
23. Vilardo, G.; De Natale, G.; Milano, G.; Coppa, U. The seismicity of Mt. Vesuvius. *Tectonophysics* **1996**, *261*, 127–138. [CrossRef]
24. Bianco, F.; Castellano, M.; Milano, G.; Ventura, G.; Vilardo, G. The Somma-Vesuvius stress field induced by regional tectonics: Evidences from seismological and meso-structural data. *J. Volcanol. Geotherm. Res.* **1998**, *82*, 199–218. [CrossRef]
25. Bruno, P.P.G.; Cippitelli, G.; Rapolla, A. Seismic study of the Mesozoic carbonate basement around Mt. Somma-Vesuvius, Italy. *J. Volcanol. Geotherm. Res.* **1998**, *84*, 311–322. [CrossRef]
26. Bruno, P.P.G.; Rapolla, A. Study of the sub-surface structure of Somma-Vesuvius (Italy) by seismic reflection data. *J. Volcanol. Geotherm. Res.* **1999**, *92*, 373–387. [CrossRef]
27. Vitale, S.; Ciarcia, S. Tectono-stratigraphic setting of the Campania region (southern Italy). *J. Maps* **2018**, *14*, 9–11. [CrossRef]
28. Vilardo, G.; Ventura, G.; Milano, G. Factors controlling the Vesuvius seismicity. *Volcanol. Seismol.* **1999**, *20*, 219–238.
29. Milia, A.; Torrente, M.M. Late-Quaternary volcanism and transtensional tectonics in the Bay of Naples, Campanian continental margin, Italy. *Mineral. Petrol.* **2003**, *79*, 49–65. [CrossRef]

30. Marinoni, L.B. Crustal extension from exposed sheet intrusions: Review and method proposal. *J. Volcanol. Geotherm. Res.* **2001**, *107*, 27–46. [CrossRef]
31. Milia, A.; Mirabile, L.; Torrente, M.; Dvorak, J.J. Volcanism offshore of Vesuvius Volcano in Naples Bay. *Bull. Volcanol.* **1998**, *59*, 404–413. [CrossRef]
32. Aiello, G.; Marsella, E.; Ruggieri, S. Three-dimensional magneto-seismic reconstruction of the 'Torre del Greco' submerged volcanic structure (Naples Bay, Southern Tyrrhenian Sea, Italy): Implications for Vesuvius's marine geophysics and volcanology. *Near Surf. Geophys.* **2010**, *8*, 17–31. [CrossRef]
33. Paoletti, V.; Passaro, S.; Fedi, M.; Marino, C.; Tamburrino, S.; Ventura, G. Subcircular conduits and dikes offshore the Somma-Vesuvius volcano revealed by magnetic and seismic data. *Geophys. Res. Lett.* **2016**, *43*, 9544–9551. [CrossRef]
34. Brocchini, D. Cronologia ed Evoluzione del Vulcanismo Nell'Area del Somma-Vesuvio. Ph.D. Thesis, Università di Pisa, Pisa, Italy, 1999; p. 167.
35. Rosi, M.; Principe, C.; Vecci, R. The 1631 Vesuvius eruption. A reconstruction based on historical and stratigraphical data. *J. Volcanol. Geotherm. Res.* **1993**, *58*, 151–182. [CrossRef]
36. Principe, C. The 1631 eruption of Vesuvius—Volcanological concepts in Italy at the beginning of the XVII century. In Proceedings of the 20th INHIGEO Symposium, Naples, Aeolian Islands, Catania, Italy, 19–25 September 1995; pp. 525–542.
37. Barbarulo, G. Le denominazioni Monterone e Tirone nella toponomastica medievale napoletana. Archivio Storico per le Provincie Napoletane. *Napoli CXXIII* **1996**, *2005*, 1–10.
38. Sorrentino, I. *Istoria del Monte Vesuvio Divisata in due Libri*; Napoli: Naples, Italy, 1734; p. 224.
39. Cerbai, I.; Principe, C. *Bibliography of Historic Activity on Italian Volcanoes. Institute of Geochronology and Isotope Geology*; Internal report n. 6/96; Italian National Research Council (IGGI): Pisa, Italy, 1996; p. 681.
40. *Allievi IGM Carta Topografica del Monte Vesuvio Rilevata e Disegnata dagli Allievi dell'Istituto Topografico Militare Negli Anni 1875-76 alla Scala di 1:10000*; Istituto Geografico Militare: Florence, Italy, 1876.
41. Johnston-Lavis, H.J. *Geological Map of Monte Somma and Vesuvius, 1:10,000, Constructed during the Years 1880–1888*; George Philip & Son: London, UK, 1891.
42. Fiechter, A. *Cono Vesuviano. Longitudine dal Meridiano di Roma (Monte Mario). Scala nel Rapporto di 1 a 10.000*; Levata nel 1900; Istituto Geografico Militare: Florence, Italy, 1904.
43. Fiechter, A. *Cono Vesuviano (dopo l'eruzione dell'Aprile 1906). Longitudine dal Meridiano di Roma (Monte Mario). Scala nel Rapporto di 1 a 10.000. Colle Ricognizioni Generali del Settembre 1906*; Levata nel 1900; Istituto Geografico Militare: Florence, Italy, 1906.
44. Arrighi, S.; Principe, C.; Rosi, M. Violent strombolian and subplinian eruptions at Vesuvius during post-1631 activity. *Bull. Volcanol.* **2001**, *63*, 126–150. [CrossRef]
45. Principe, C.; Brocchini, D. Fracturation pattern at Vesuvius during the 1631–1944 period. *Per. Mineral.* **1995**, *64*, 255–256.
46. Alfano, G.B. La successione dei crepacci eruttivi sui fianchi del Gran Cono Vesuviano. *Bull. Volcanol. Napoli Année* **1925**, *2*, 277.
47. Sevink, J.; van Bergenb, M.J.; van der Plichtc, J.; Feikend, H.; Anastasia, C.; Huizingab, A. Robust date for the Bronze Age Avellino eruption (Somma-Vesuvius): 3945 10calBP (1995 10calBC). *Quat. Sci. Rev.* **2011**, *30*, 135–146. [CrossRef]
48. Di Renzo, V.; Di Vito, M.A.; Arienzo, I.; Carandente, A.; Civetta, L.; D'Antonio, M.; Tonarini, S. Magmatic history of Somma-Vesuvius on the basis of new geo-chemical data from a deep bore-hole (Camaldoli della Torre). *J. Petrol.* **2007**, *48*, 753–784. [CrossRef]
49. Cinque, A.; Irollo, G. Il "Vulcano di Pompei": Nuovi dati geomorfologici e stratigrafici. *Il Quat.-Ital. J. Quat. Sci.* **2004**, *17*, 101–116.
50. Sulpizio, R.; Cioni, R.; Di Vito, M.A.; Mele, D.; Bonasia, R.; Dellino, P. The Pomici di Avellino eruption of Somma-Vesuvius (3.9 ka BP). Part I: Stratigraphy, compositional variability and eruptive dynamics. *Bull. Volcanol.* **2010**, *72*, 539–558. [CrossRef]
51. Nilsson, M. Evidence of Palma Campania settlement at Pompei. In *Nuove Ricerche Archeologiche Nell'Area Vesuviana (scavi 2003–2006)*; Guzzo, P.G., Guidobaldi, M.P., Eds.; Diva Portal: Södertörn, Sweden, 2008; pp. 81–86.
52. Senatore, M.R.; Ciarallo, A.M.; Stanley, J.-D. Pompeii Damaged by Volcaniclastic Debris Flows Triggered Centuries Prior to the 79 A.D. Vesuvius Eruption. *Geoarchaeology* **2014**, *29*, 1–15. [CrossRef]
53. Le Hon, H.S. *Carte Topographique des Laves du Vesuve, a l'echelle de 1/25.000, 1631–1861, Avec la Coupe Geologique du Rivage Napolitan*; Muquardt, L.C., Detken, N.A., Eds.; C. Muquardt: Bruxelles, Belgium, 1866.
54. Di Girolamo, P. Rilevamento petrografico-stratigrafico lungo il margine SW del Vesuvio (manifestazione eruttiva locale e colate di fango del 79 d.C.). *Rend. Soc. Ital. Mineral. Petrogr.* **1970**, *XXVI*, 77–108.
55. Andronico, D.; Cioni, R. Contrasting styles of Mount Vesuvius activity in the period between the Avellino and Pompeii Plinian eruptions, and some implications for assessment of future hazards. *Bull. Volcanol.* **2002**, *6*, 372–391. [CrossRef]
56. Principe, C.; Paolillo, A.; La Felice, S.; Arrighi, S. Forma Vesuvii—2 Volcanic morphology at the time of the 79 AD Plinian eruption. *Physis* **2021**, *LVI*, 289–302.
57. Johnston-Lavis, H.J. The geology of the Mt. Somma and Vesuvius: Being a study of Volcanology. *Q. J. Geol. Soc. Lond.* **1884**, *40*, 35–149. [CrossRef]
58. Johnston-Lavis, H.J. *A Short and Concise Account of the Eruptive Phenomena & Geology of Monte Somma and Vesuvius in Explanation of the Great Geological Map of that Volcano*; George Philip & Son: London, UK, 1891; p. 24.
59. Rolandi, G.; Petrosino, P.; Mc Geehin, J. The inter-plinian activity at Somma-Vesuvius in the last 3500 years. *J. Volcanol. Geotherm. Res.* **1998**, *82*, 19–52. [CrossRef]

60. Cioni, R.; D'Oriano, C.; Bertagnini, A.; Andronico, D. The 2nd to 4th century explosive activity of Vesuvius: New data on the timing of the upward migration of the post-A.D. 79 magma chamber. *Ann. Geophys.* **2013**, *56*, S0438. Available online: https://www.annalsofgeophysics.eu/index.php/annals/article/view/6444 (accessed on 14 January 2024).
61. Sulpizio, R.; Mele, D.; Dellino, P.; La Volpe, L. A complex, Subplinian-type eruption from low-viscosity, phonolitic to tephri-phonolitic magma: The AD 472 (Pollena) eruption of Somma-Vesuvius, Italy. *Bull Volcanol* **2005**, *67*, 743–767. [CrossRef]
62. Principe, C. Le Eruzioni Storiche del Vesuvio: Riesame Critico, Studio Petrologico dei Prodotti ed Implicazioni Vulcanologiche. Ph.D. Thesis, University of Pisa, Pisa, Italy, 1979.
63. Carta, S.; Figari, R.; Sassi, E.; Sartons, G.; Scandone, R. A statistical model for Vesuvius and its volcanological implications. *Bull. Volcanol.* **1981**, *44*, 121–151. [CrossRef]
64. Scandone, R.; Giacomelli, L.; Fattori Speranza, F. Persistent activity and violent strombolian eruptions at Vesuvius between 1631 and 1944. *J. Volcanol. Geotherm. Res.* **2008**, *170*, 167–180. [CrossRef]
65. Bonasia, V.; Del Pezzo, E.; Pingue, F.; Scandone, R.; Scarpa, R. Eruptive history, seismic activity and ground deformations at Mt. Vesuvius, Italy. *Ann. Geophys.* **1985**, *3*, 395–406.
66. Hobbs, W.H. The Grand Eruption of Vesuvius in 1906. *J. Geol.* **1906**, *14*, 636–655. Available online: https://www.jstor.org/stable/30078588 (accessed on 14 January 2024).
67. Johnston-Lavis, H.J. The Eruption of Vesuvius of June 7, 1891. *Nature* **1891**, *44*, 320–322. [CrossRef]
68. Zurcher, F.; Margollé, É. *Volcanoes and Earthquakes*; Philadelphia, J.B., Ed.; Lippincott & Co.:: London, UK, 1869; p. 253.
69. Principe, C.; Rosi, M.; Santacroce, R.; Sbrana, A. Chapter 1. Explanatory notes to the geological map. In *Somma-Vesuvius*; Santacroce, R., Ed.; Quaderni de 'La Ricerca Scientifica' CNR: Rome, Italy, 1987; Volume 114, pp. 11–52.
70. De Bottis, G. *Ragionamento Istorico Intorno a' Nuovi Vulcani Comparsi Nella Fine Dell'Anno Scorso 1760 nel Territorio della Torre del Greco*; Napoli, Di Simone: Naples, Italy, 1761; p. 58.
71. Breislak, S.; Winspeare, A. *Memoria Sull'Eruzione del Vesuvio Accaduta la Sera dè 15 Giugno 1794*; Napoli: Naples, Italy, 1794; p. 89.
72. Principe, C. The 1794 flank eruption of Vesuvius (Italy)—Phenomenology, Volcanological and Social Impact. In Proceedings of the Abstract IUGG 28th General Assembly, Berlin, Germany, 11–20 July 2023.
73. Palmieri, L. Intorno all'incendio del Vesuvio cominciato il dì 8 dicembre 1861. *Rend. Tornate Dell'accademia Pontiniana Anno Decimo* **1862**, *40–61*, 72–83. [CrossRef]
74. Forbes, D. The Eruption of Vesuvius in 1872. *Nature* **1873**, *7*, 259–261. [CrossRef]
75. Stoppa, F.; Principe, C.; Schiazza, M.; Giosa, P.; Liu, Y.; Crocetti, S. 1631 Magma evolution inside the 1631 Vesuvius magma chamber and eruption triggering. *Open Geosci.* **2017**, *9*, 24–52. [CrossRef]
76. Neri, A.; Aspinall, W.; Cioni, R.; Bertagnini, A.; Baxter, P.J.; Zuccaro, C.; Andronico, D.B.S.; Cole, P.; Esposti Ongaro, T.; Hincks, T.; et al. Developing an Event Tree for probabilistic hazard and risk assessment at Vesuvius. *J. Volcanol. Geotherm. Res.* **2008**, *178*, 397–415. [CrossRef]
77. Marzocchi, W.; Sandri, L.; Gasparini, P.; Newhall, C.; Boschi, E. Quantifying probabilities of volcanic events: The example of volcanic hazard at Mount Vesuvius. *J. Geophys. Res.-Solid Earth* **2004**, *109*, 1–18. [CrossRef]
78. Marzocchi, W.; Newhall, C.; Gordon, W. The scientific management of volcanic crises. *J. Volcanol. Geotherm. Res.* **2012**, *247*, 181–189. [CrossRef]
79. Scandone, R.; Giacomelli, L.; Gasparini, P. Mount Vesuvius: 2000 years of volcanological observations. *J. Volcanol. Geotherm. Res.* **1993**, *58*, 5–25. [CrossRef]